Plastic Limit Analysis of Earthbag Structures

Student: Ralph Pelly
Supervisor: Dr Andrew Heath

Department of Architecture and Civil Engineering
The University of Bath
2009

AR40223 MEng dissertation

Abstract

In this paper, a detailed experimental analysis is carried out of the strength and structural performance of earthbag construction. An attempt at modelling the behaviour of earthbag arches using masonry arch plastic limit analysis is made, and conclusions drawn regarding its applicability to this method of construction.

The relatively short history of earthbag construction is reviewed, and particular reference made to a planned earthbag dome project in the Namib Desert, Namibia. Constituent materials of polypropylene bags and sandy fill material are used to match expected conditions on this project, and material properties are defined in a series of tests. The compression strength, stiffness and friction coefficient of the earthbags are determined and used in further analysis on the structural system.

Earthbag arches are tested, and it is shown that earthbag structures undergo large plastic deformations before ultimate collapse, and that properties can be improved significantly through the stabilisation of fill material. It is concluded that plastic limit analysis is appropriate only where stabilised fill material is employed.

Acknowledgements

I would like to give my sincerest thanks and appreciation for all the support and advice I have received from so many people, not just in writing this paper but in studying for my degree over the last four years. It would not have been possible without them:

Will Bazeley, Neil Price, Brian Purnell and Sophie Hayward, for their tireless and enduringly positive support through the entire experimental programme.

Nicola du Pisanie, Tim Mander, and everyone at Integral Engineering Design, who have given so much of their expert time and advice to the project.

Dr Andrew Heath has been an exceptionally friendly and supportive supervisor, and his door is always open. Also Mark Evernden has provided much knowledgeable advice and support.

My thanks also to Nikul Vadgama, for being a great partner, whose hard-work and commitment has enabled him to put up with me for four years.

And finally to Laura, for so many things.

Table of Contents

List of Figures

List of Tables

List of symbols

$\boldsymbol{B}$	Bag width
$\boldsymbol{B_f}$	Bag width at failure
$\boldsymbol{c}$	Effective cohesion
$\boldsymbol{F}$	Applied vertical force
$\boldsymbol{H}$	Bag thickness
$\boldsymbol{H_f}$	Bag thickness at failure
$\boldsymbol{L}$	Bag length
$\boldsymbol{L_f}$	Bag length at failure
$\boldsymbol{R_i}$	Radius of curvature to point i
$\boldsymbol{T}$	Tension force in bag material
$\boldsymbol{w}$	Earthbag weight
$\boldsymbol{\sigma_x}$	Total horizontal stress
$\boldsymbol{\sigma_{x,ex}}$	Horizontal stress due to externally applied horizontal load
$\boldsymbol{\sigma_{x,t}}$	Horizontal stress due to bag material tension force
$\boldsymbol{\sigma_y}$	Total vertical stress
$\boldsymbol{\sigma_{y,ex}}$	Vertical stress due to externally applied vertical load
$\boldsymbol{\sigma_{y,t}}$	Vertical stress due to bag material tension force
$\boldsymbol{\sigma_1}$	Major principal stress
$\boldsymbol{\sigma_3}$	Minor principal stress
$\boldsymbol{\theta_i}$	Angle from vertical to point i
$\boldsymbol{\varphi}$	Internal angle of friction

1 Introduction

Sandbags (otherwise known as earthbags or soilbags, depending on the application) are hessian or polypropylene bags that, since their invention in the 17th century for fortifying military defences, have become ubiquitous through their prolific use in a wide variety of fields, such as flood protection and earth retaining systems. Their ability to be lifted by hand makes them versatile and manageable, and they can be filled with any granular material suitable for the particular application. In the geotechnical field they are usually known as soilbags, and are used in a number of applications to control settlement and increase soil strength (Matsuoka and Liu, 2006). They have also been used in small-scale structures, both as non-structural and structural components, where they are called - and will be referred to in this dissertation as - 'earthbags'.

Figure 1.1: Earthbag construction project in India (Anon, 2007).

This dissertation is concerned with the use of earthbags as a structural element in buildings formed wholly of earthbags, in a building method known as flexible form rammed earth. This work will attempt to develop a greater understanding of the behaviour of earthbag structures and explore the feasibility and limits of this building method. Currently the main source of knowledge on earthbag structures is from trial and error and past experience. This will build on the limited research carried out in this field to date, and help inform design of future projects.

Particular reference will be made to a proposed project to build earthbag structures in the Namib Desert by Feilden Clegg Bradley Studios. Expected conditions on this project will be used to help inform experimental parameters, due to the lack of precedent in this field of research, and to give experimental findings relevance and comparability to real world scenarios. This project will be discussed in more detail in Chapter 3.

Testing of full 3 dimensional structures exceeds the limits of time and resources available for this project, therefore testing will be limited to a 2 dimensional arch form. The structure will be analysed using a masonry arch plastic limit analysis model, and experimental results will be compared with model predictions, to explore the applicability of the model to this building method.

This dissertation will gain information on the strength and stiffness of earthbag structures, and explore their overall behaviour and critical failure modes in a methodological way, which will build on the existing practical knowledge of earthbag structures, and form a foundation for future academic research on the subject. Work by Vadgama (2010) compliments and builds on from this paper, focusing particularly on material properties and variability.

2 Literature review

2.1 Description of Earthbag Structures

Flexible form rammed earth is a building method consisting of filled earthbags laid in courses like a masonry structure, usually in a running bond. Barbed wire is laid between the courses to provide shear resistance. This system has no tensile strength, so structures must be built into compression forms, such as domes and arches, often resulting in a structure that resembles an igloo, as seen in Figure 1.1. By building in this way, the entire structure can be made from earthbags, with no need for a separate roof structure to span between walls. The shape of these structures means that they are self-supporting throughout construction hence can be built without centring. Formwork is required in door and window voids, and earthbags can be laid to span across in an arch. The practicalities of building an earthbag structure are dealt with in detail by Hunter and Kiffmeyer (2004).

2.2 Development of Earthbag Structures

The use of earthbag structures has been explored in a number of situations, where their unique set of attributes give them the potential to provide an efficient and fitting solution. Possibly the first experimentation of the flexible form rammed earth building method was conducted by Gernot Minke in 1977, in developing a low cost, earthquake resistant building method using natural building materials in Guatemala (Grasser and Minke, 1990). A structural wall system was devised using hessian or cotton tubes filled with crushed pumice stone, stacked between thin bamboo poles for stability (see Figure 2.2). He also built a test dome in Kassel, Germany, using polyester hoses filled with earth, shown below in Figure 2.1 (Minke, 2006). This inverted catenary shape was achieved with the aid of a rotating arm mounted in the centre of the dome.

Figure 2.1: Minke's earthbag dome, built in 1977, still standing in 1997 (Grasse and Minke, 1990).

It was found that the use of bags for packing and confining the material negated the need for binders such as cement, resulting in significant savings in material costs. Compared to a similar house built using cement blocks, the material cost was reduced by half. Pumice was used in the Guatemalan construction due to its lightweight and enhanced thermal insulation properties compared to other bulk material. The cotton tubes were coated with lime paint to protect the material from rotting and to stabilize and waterproof the surface. The high ductility of the structure was expected to provide very good earthquake resistance (Minke, 2006).

Figure 2.2: Construction of structural earthbag wall system in Guatemala, 1977 (Grasser and Minke, 1990).

The figure that helped to popularize earthbag structures more than any other was Nader Khalili, who first proposed their use for colonizing the moon, where the use of unprocessed, insitu materials would minimise the costly transport of material and energy from earth (Khalili, 1990). He further refined the idea into a system called 'superadobe' (Khalili and Vittore, 1998), which incorporates long filled polyester tubes laid with barbed wire between the courses, to provide shear resistance and add stability to the structure. Using continuous tubes can also give hoop strength to the dome, and reduce the labour intensity of the construction process, as the tubes are filled insitu. He argued that one of the benefits of earthbag domes is their ability to be self-supporting during construction, minimising the amount of timber required.

Superadobe domes have been used as emergency shelter in disaster situations, due to the availability of constituent materials, short construction times, and limited requirement for skilled labour, which is always in short supply at such times (Khalili, 2008). Because they often contain no cement, there is no delay to construction associated with stabilisation. Structures can be temporary, or can be rendered to protect the polyester bags from UV degradation, which will increase their longevity. These structures were used in the rehabilitation response to the October 2005 earthquake in Pakistan (Trivedi, 2002), where their thermal mass helped to dampen the large diurnal temperature range – something that the refugee tents typical of these situations are unable to do.

Other proponents of earthbag structures cite the sustainable credentials of the building method (Hunter and Kiffmeyer, 2004). The bulk of the material is simply earth which is taken from onsite, and the domes are constructed entirely by hand, giving them extremely low embodied energy compared to most other traditional building methods.

Khalili founded the California Institute of Earth Art and Architecture in 1991 to "research, develop and teach the technologies of Ceramic Houses and Superadobe, by building, testing and designing prototypes" (Cal-Earth, 2010). They have held training courses to teach people how to build earthbag structures, and provide information such as typical structural plans to prospective builders, working with the local council in California to gain building code approval for this method of construction. They report to have conducted multiple experiments on test domes to verify the strength and performance of earthbag structures above and beyond American building code requirements, but have not to date published any articles on the subject.

2.3 Existing Research

2.3.1 Cal-Earth

Limited details of two tests on an earthbag dome are reported by Harp and Regner of Hesperia City Council, California (Khalili and Vittore, 1998). A static test and a dynamic test were carried out by engineers to test the structures in relation to wind loading, live loading and earthquake loading. Sandbags were placed on one third of the dome to a weight of 3.9kN/m^2 during the static test, and deflection was monitored. It is reported that "there was no movement of any surface of [the] dome structure as a result of the loading described in the test procedure." (Khalili and Vittore, 1998). During the dynamic test, a rig was set up to apply and relax loads over a short period of time according to the most stringent seismic loading limits stipulated for California Seismic Zone 4. The magnitude of load applied is not specified, nor is the size of the dome tested, but it is reported that required limits were greatly exceeded until the testing apparatus began to fail, and that throughout this experiment, no deflection or failure of the structure was noted.

The failure of the testing rig, lack of any deflection data regarding the dome and lack of any publicly available results all brings into question the quality of tests carried out. Unfortunately, this is largely representative of the quality of testing carried out to date on earthbag structures. The structural system remains a niche method, practiced by a small number of individuals on small scale projects, with information shared informally within the community. Due to the nature of the typical project, where lack of resources is the key driver, more emphasis is placed on the practicalities of building an earthbag structure, and the knowledge of their strength and stability is predominantly achieved through trial and error and prior experience.

2.3.2 Other Parties

Two independent bodies of research have been carried out, specifically related to determining the strength of earthbags. A short study on the compressive strength of earthbags was carried out by Dunbar (2006).

The study investigated the compressive strength of polypropylene bags stacked 3 bags high, filled with 'rubble', sand and 'dirt'. The failure strength of the bags, defined as the load at which initial tearing of the bag material occurred, was reported as 0.4 MPa, 0.3 MPa and 2.1 MPa respectively. However, no tearing was observed in the dirt-filled bag tests, as the capacity of the testing equipment was reached before failure occurred. The sand-filled specimens gained strength after initial failure had occurred, reaching a peak strength of 0.66MPa, whereas the rubble-filled specimens lost all significant strength upon failure of the bag material.

The exact composition of the fill material was not discussed, but it was suggested that coarser, angular particles produce tearing of the bags at lower loads. The failure mode observed was tearing of the bag material in two parallel lines on the top and bottom face of the middle bag, running longitudinally the length of the face. The material described as dirt presumably contained a certain proportion of organic material, as the dirt-filled specimens experienced a stiffness approximately ten times lower than that of the other materials. It was noted that deflection rather than strength may be the more relevant limit state for earthbag structures.

This avenue of research was built on by Daigle (2008), who conducted a compressive investigation into the compressive strength of earthbag stacks under vertical load. The work considered the effect of a variety of fill types, stack heights and bag sizes.

Medium and small bag sizes were tested, with the small bag size of approximately 457mm x 762mm when empty, corresponding to the most commonly used size in earthbag construction. Relative to

their sizes, the small specimens were found to achieve a slightly higher strength, but the difference in strengths was not great.

Bags were tested filled with coarse granular material (gravel) and fine granular material (sand). Strength recorded in the 3 bag tests most similar to those carried out by Dunbar, found higher failure strengths of 1.10 MPa to 2.98 MPa for gravel filled specimens, and 2.33 MPa to 2.98 MPa for sand filled specimens. It was found that stack heights of 3 bags could exaggerate strengths, due to the confinement of the bag material caused by the plates above and below the specimen. Stacks heights of 3, 6 and 9 bags were tested, and strength was found to be inversely proportional to stack height.

A number of limitations exist that affect the quality of results obtained from these tests. Significantly, the upper strength values of 2.98MPa do not relate to the behaviour of the specimens, but represent the capacity of the testing equipment. Therefore, failure of some of the specimens was not achieved. The direct comparison of strength results to the work by Dunbar is perhaps inappropriate, as in Daigle's tests, failure was defined as a loss of fill resulting in reduced compressive load bearing capacity. This is a rather more onerous definition than Dunbar's, and explains why the strengths found were so much higher.

Fine grained material filled bags were found to be stronger and stiffer than gravel filled bags. The results suggested that earthbag wall ultimate strength – of 122-144kN/m for gravel filled bags, and 1123-1327kN/m for sand filled bags – compares favourably with other wall construction methods. This is partly due to their greater width, but it is again suggested that overall stability and stiffness, rather than ultimate strength, may be the more critical factor in determining the suitability of earthbag structures in construction.

Daigle's work also attempts to address the lack of standard methodologies for testing earthbags, by wherever possible basing his methods on standards used for similar materials, such as masonry, and where that is not possible by replicating as closely as possible the expected conditions observed on earthbag construction projects. Daigle notes that:

"Unfortunately, while anecdotal knowledge on earthbag construction has been well developed over the past thirty years, this has not been matched by efforts to study the material in a quantitative fashion consistent with other structural engineering materials. As such, the practice of earthbag construction is currently based on many "rules of thumb" and unsubstantiated best practices which, while well meaning, may not result in the safest, most efficient use of materials." (Daigle, 2008)

2.4 Research on earthbags in other fields

Research on earth filled bags has also been carried out in other fields, and some of the findings from these studies may be applied usefully to earthbag structures.

In the field of soil reinforcement, some research has been conducted on the relatively recent idea of using earth filled bags (called soilbags) to significantly increase the bearing capacity of soft soils and reduce settlements (Xu *et al*, 2008). Matsuoka and Liu (2006) lists some of the main benefits of using soilbags as:

- Bags are cheap and easily available.
- Fill material can be a variety of construction waste material, thereby contributing to site recycling.
- No special construction equipment is required – bags can be manipulated by hand.
- The use of cement and chemical agents is avoided, making soilbags a sustainable option.

They also suggest that one of the reasons soilbags haven't been adopted more widely for use in permanent applications is their vulnerability to UV degradation.

Xu *et al* (2008) describe a method of earth reinforcement using soilbags, and investigate their strength properties using unconfined compression tests on bags filled with gravels or medium grained sands. Testing shows that the compressive strength of soilbags is related to the tensile strength of bag material, and internal angle of friction of fill material. Compressive strength is high, due to the mobilization of tensile forces in the bag material causing increasing confinement of the soil. The tensile properties of a polypropylene bag material, equivalent to those used in earthbag construction are obtained. The average strength is measured as 23.7kN/m and maximum tensile strain as 12.6%.

Compression tests are carried out on individual bags, filled with gravel or medium grained sand, and strengths are found to be 2.1MPa and 1.6MPa respectively. The bags were observed to tear at contact points with the loading plates and along seams. Strain at failure was also measured as 45% and 48% respectively, and the stiffness of the bags was observed to increase as the test progressed, suggesting that settlement of the fill material occurs initially at a lower stiffness, the subsequently the confinement of the soil due to tension in the bag material increases, increasing stiffness.

The authors conclude that gravel filled bags have a higher compressive strength due to their higher internal angle of friction, but the comparison between the two fill types is not necessarily accurate, as the gravel filled bags were significantly smaller, and therefore achieved a lower failure load than the sand specimens. It is not stated categorically in the paper, but is likely that failure of the bags was defined as the load at which initial tearing of the bag material occurred. This puts the strength results from these tests above those found by Dunbar, who used a similar definition of failure. However it must be noted that tests were conducted on individual bags, which is expected by Daigle to significantly increase compressive strength results due to the confinement from loading plates. Daigle also noted that premature failing of gravel filled bags occurred through tearing of bag material at interfaces between 2 bags, which could contribute to the discrepancy between values. Considering the number of variables involved, such as exact composition of fill and bag material, and the difficulty in controlling the material accurately, these strength results are of the same order of magnitude as Dunbar and Daigle, and therefore demonstrate some consistency in test methodology.

Xu *et al* (2008) go on to describe the relationship between soilbag compressive strength and bag material tensile strength, discussed in further detail in Chapter 5.1. The theoretical values calculated by this method correlated very well with their experimental results. The stress-strain relationship of soilbags under axial compression was also modelled, again matching experimental data well. It was found that the stress-strain relationship of soilbags differs from that of insitu soil.

2.5 Analysis of masonry or stone block structures

As stated above, the behaviour of earth filled bags can share similarities with soil behaviour, i.e. the fill material in the bag. But earthbags can also possess similarities to masonry blocks, because of their similar block-like nature. Compression strength tests will tend to make them exhibit soil-like behaviour, as the shape of the bag is being deformed, and earth pressures are mobilized. However, in an earthbag structure, stresses are not likely to become high enough to achieve this level of deformation, and therefore earthbags may act relatively like a rigid block, such as masonry. In this case, it is shear strength of bag interfaces, and geometrical effects that are likely to govern strength and stability. It is therefore sensible to consider how similar masonry structures are analysed, in order to determine how best to analyse earthbag structures.

Unsurprisingly due to the number of masonry structures currently in use throughout the world, very much greater study has been directed towards them than to earthbags. Many traditional masonry buildings consist of arches, vaults and domes, and it is these forms that are of particular interest.

2.5.1 Masonry Arches

Heyman (1995) first developed the use of plastic analysis for masonry arches, which has since become widespread. He described the stability of a masonry arch as a purely geometrical problem, and stated that stability was dependent on the line of thrust of the arch lying wholly within the depth of the voussoirs. There may be more than one equilibrium solution for a given problem, but according to the safe theorem of plasticity, if one theoretical condition can be found that is safe, then the actual condition is also safe (Sinopoli, 1998). Heyman lists the initial assumption used in this method of analysis:

- Masonry has no tensile strength.
- Masonry has infinite compressive strength
- Blocks are rigid.
- Sliding failure does not occur.

Further assumptions have also been stated by Gilbert and Melbourne (1994):

- Strains are small, and therefore cause negligible changes to the geometry of the arch.
- Blocks initially fit perfectly together.

Clearly some of these assumptions correspond well to the expected behaviour of earthbag structures, and some may not be accurate. One point to consider is that the plastic method of analysis does not consider material properties of the masonry or stone other than the self-weight, and can therefore be applied to any material for which material properties may not be well defined, such as earthbags. The application of earthbags to this method of analysis will be examined in further detail in Chapter 6.1.

Some of the assumptions stated above have been considered in more detail by subsequent studies. For instance, Livesley (1978) and others, have introduced finite frictional resistance between the arch blocks, enabling sliding failure to be considered. Commercial software packages, such as Ring 2.0 (LimitState, 2009) allow analysis of arch structures to be computerised, taking into consideration sliding failure, and crushing failure of voussoirs.

3 Earthbag Domes in Namibia

The nature of earthbag is such that with each new project, the unique conditions presented by the site are likely to create a level of uncertainty at the design stage as to the material properties of the earthbags, and performance of the earthbag structures built using the particular set of constituent materials present. The limited body of knowledge surrounding earthbag structures means that these questions can be difficult to answer to a great degree of certainty from existing research and past experience alone. In contrast, carrying out research in the field of earthbag structures, it can be difficult to decide exactly how tests should be carried out, and what materials should be used, due to the lack of guidelines and the individual nature of earthbag projects.

Therefore, by carrying out research in tandem with a developing real world project, the research can be informed by the particular conditions found on the project, and can then inform the project in turn. This investigation makes reference to a project to design and build an earthbag hub in the Namib Desert, Namibia. It is hoped that this will help to inform testing procedure, and give relevance to the results and conclusions from this work.

3.1 Project Description

Figure 3.1: A half-built timber framed Topnaar dwelling, surrounded by desert sand.

Feilden Clegg Bradley Studios are working in Collaboration with the Bastos Foundation based in Namibia, to empower a local community, through knowledge transfer and providing skills and resources, to improve their built environment by considering a new and alternative building method.

The Topnaar community are an indigenous people living on the banks of the Kuiseb River in northern Namib Desert, Namibia. Being descended originally from nomadic tribes, they have no vernacular architecture to draw on (du Pisanie, 2009), and currently live in driftwood framed houses, clad in corrugated iron sheeting. The houses are all self-built over a period of a few years, as the driftwood must be sourced from the ephemeral Kuiseb River each rainy season. The corrugated iron is then sourced from Walvis Bay, at a distance of 2 hours drive and a cost of around $40/sheet. While these dwellings follow the western convention of being rectilinear, they do not respond to the local environment of the Namib Desert, and can provide very uncomfortable living conditions. There is a very high diurnal temperature range of 20-30° (von Willert, 1992), and with total lack of thermal control afforded by the iron sheet cladding, internal temperature have been found to be 5-7° hotter than the external temperature during the heat of the day (du Pisanie, 2009), and cold at night.

3.1.1 Response

A proposal has been put forward by Feilden Clegg to demonstrate to the Topnaar an alternative building method that will improve their built environment and living conditions by responding to the local climate, and being appropriate for the resources available. Earthbag structures have been singled out as being particularly applicable to the situation for a number of reasons, many of which have been described earlier:

- **Thermal performance** – A large mass and thick walls prevent heat from travelling quickly across the thickness of the wall, damping the large diurnal temperature fluctuations. The interior remains cooler during the day as the building fabric absorbs heat, and warmer at night as that heat is re-emitted.
- **Availability of materials** – The fill material used in earthbag structures can be taken literally from the ground beneath your feet. Being so sparsely populated, earth is in no short supply in the Namib Desert. Sandbags and barbed wire are ubiquitously available across the globe.
- **Buildability** – Earthbag structures do not require specialist tools or especially skilled labour, so can be built by the Topnaar with simple tools and a minimal amount of instruction.
- **Affordability** – Because the earth and labour are effectively free, the main cost is that required for materials such as barbed wire, sandbags and timber to be used as formwork, all of which are relatively cheap, and the timber formwork can be reused multiple times.
- **Durability** – Once rendered, the sandbag material is protected from UV degradation, and the large mass and high plasticity of the overall structure provides a high level of durability and ability to withstand impact loading.

A demonstration build will be conducted as a community project, involving volunteers from each of the local Topnaar villages. The resulting earthbag hub will act as a showcase for the building method, and the construction programme will provide the knowledge and skills transfer to allow the local people to continue building earthbag structures for themselves, should the project prove a success and earthbag structures be accepted by the local community as something that can improve their quality of life.

3.2 Local Conditions

Test parameters will be chosen to match expected local site conditions as closely as possible, to give real-world relevance to the results, to help inform project design and reduce the large number of variables involved in earthbag structures for the purpose of simplifying the experimental programme.

3.2.1 Fill Material

The fill material used throughout the testing programme is medium grained sand, with particle distribution chosen to match that of the Namibian sand that will be used on this project. The particle distributions of the two soils are shown in Figure 3.2. Earthbag structures are more commonly constructed using a fill material with at least 10% fines, to aid compaction (Hunter and Kiffmeyer, 2004). Clays are not present in significant quantities on site, therefore the analysis of the performance of the proposed structures is vital.

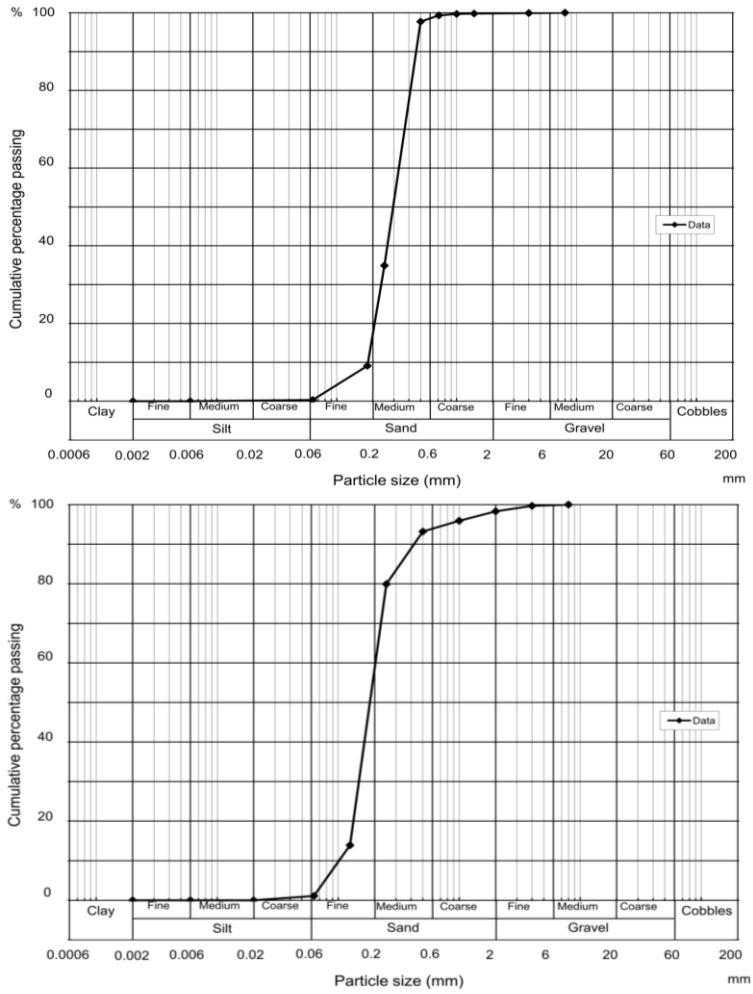

Figure 3.2: Graphs comparing particle size distribution of Namibian sand and sand used in experimental programme.

3.2.2 Bag Size

The more widely available polypropylene bags will be sourced over hessian, for their increased use-ability and durability. The ideal bag weight has been identified by the project team as 20kg, which allows for individual handling. These conditions will be matched in this investigation, and bag dimensions after tamping have been measured and approximated as shown below in Figure 3.3. Due to the natural variation and irregularity in earthbag shapes, average, approximate dimensions were required for use in analysis and calculations. The small curvatures at the bag edges were ignored, and bag length was taken as the average length between the edges and the centre of the bag.

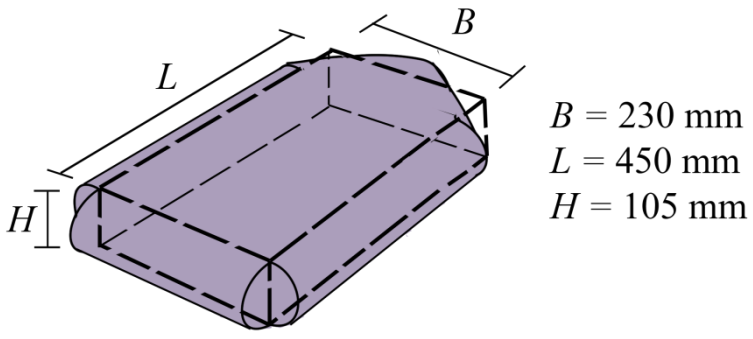

Figure 3.3: Approximation of earthbag dimensions.

4 Material Properties

In order to analyse earthbag structures, it is necessary to determine their constituent material properties, and to gain an understanding of how these properties contribute to the overall behaviour of the earthbags. The behaviour of an earthbag is determined by the properties of both the bag material and the fill material. It is most likely that these constituent material properties are going to be unique for each individual earthbag project, because the soil used as fill material can vary widely, and is usually specific to the project site. The bags themselves are also likely to come from whichever manufacturer can supply locally, and there are no specific requirements for the bag material properties, not least because they are not usually used for structural purposes. There can therefore be no established standard earthbag behaviour, and should the material properties be desired, they must be determined experimentally.

Soil shearbox tests, bag material tensile tests and earthbag shear tests were carried out in order to determine what are considered to be the most critical material properties for the behaviour of earthbag structures.

4.1 Soil Shearbox Test

The shear strength and friction angle of soil samples was determined by direct shear in the small shearbox apparatus, in accordance with clause 4 of BS 1377-7 (1990). The samples tested were dry; although moisture content of soil used varied throughout the testing programme, a drained analysis of effective shear strength is appropriate for sand.

Sample dimensions were 100mm x 100m x 47mm, and applied normal loads were applied of 314N, 804N and 1295N, corresponding to normal stresses of 31.4kN/m^2, 80.4kN/m^2 and 129.5kN/m^2. Samples were also prepared with three different levels of pre-compaction, or 'tamping' – loose, semi-tamped and tamped. This was to determine how the soil properties may be affected by tamping of the bags.

The test proceeded at a shear displacement of 1mm/min, and shear displacement, normal displacement and shear force were measured at a rate of ten times per second.

4.1.1 Results

Table 4.1: Soil Shearbox Friction Angle.

Pre-compaction	Average Bulk Unit Weight (kN/m^3)	Cohesion (kN/m^2)	Friction Angle (°)
Loose	13.80	1.67	25.87
Semi-tamped	15.49	6.00	25.78
Tamped	15.9	15.9	26.43
		Average:	26.03

Figure 4.1 shows the peak shear stress achieved for each sample, with linear trends for each level of tamping indicated. The angle of the gradient of each linear trend is the friction angle of the samples, and the y-intercept is the effective cohesion; both shown in Table 4.1. Table 4.1 shows that increased tamping increased the density of the sample, as is to be expected. The friction angle of the soil is independent of density.

Figure 4.2 shows the variation of shear stress with shear displacement of the three samples undertaken at 7kN applied normal load. This shows the higher peak stress achieved by the tamped specimen, and that all specimens reach the same residual shear stress after the shear plane is established.

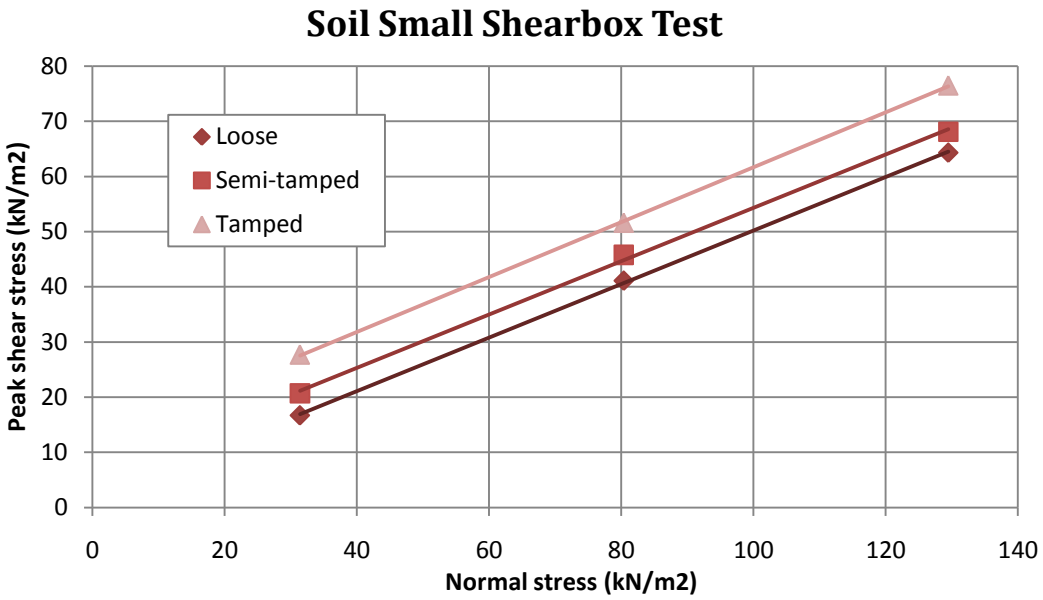

Figure 4.1: Graph showing peak shear stress against normal stress.

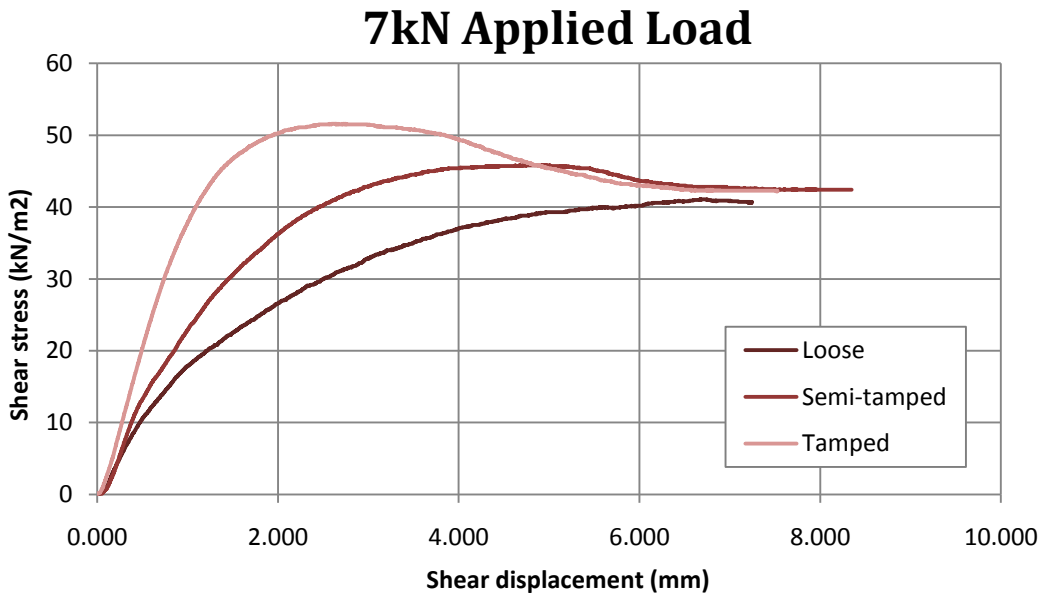

Figure 4.2: Graph showing shear stress varying with shear displacement for samples with 7kN normal load applied.

4.2 Tensile Test

The tensile strength and failure strain of the polypropylene bag material were determined by tensile tests in a Dartec 20T testing frame. Three similar tests were conducted according to BS 13934-1 (1999), on 30mm wide samples consisting of 12 longitudinal fibres. Testing proceeded at 5mm/min and applied load and extension were measured at 1 second intervals.

4.2.1 Results

Table 4.2: Bag Material Tensile Test Results.

Repeat	Tensile Strength (kN/m)	Failure Strain (%)
1	18.61	15.0
2	16.67	10.9
3	20.94	16.3
Average	18.74	14.0

Table 4.2 shows the tensile strength of each sample, and the average strength of 18.74kN/m length of bag material. Peak tensile force was reached before the first fibre was snapped, and initial specimen width was used to calculate tensile strength per unit bag length.

4.3 Earthbag Shearbox Test

The friction coefficient of the earthbag interfaces was determined by direct shear in a large shearbox apparatus, using a procedure similar to that described in clause 5 of BS 1377-7 (1990). The procedure was adjusted for using filled earthbags rather than soil samples.

Bags were filled sufficiently to be tamped in place, inside the shearbox, to form a flat rectangular area of contact of 230mm x 300mm. Insitu tamping was given to the bags to replicate earthbag structure conditions. Short 6mm diameter bars were placed between the shear boxes to act as rollers, reducing the friction caused by the apparatus and creating enough separation between each shearbox for the bag interface to shear.

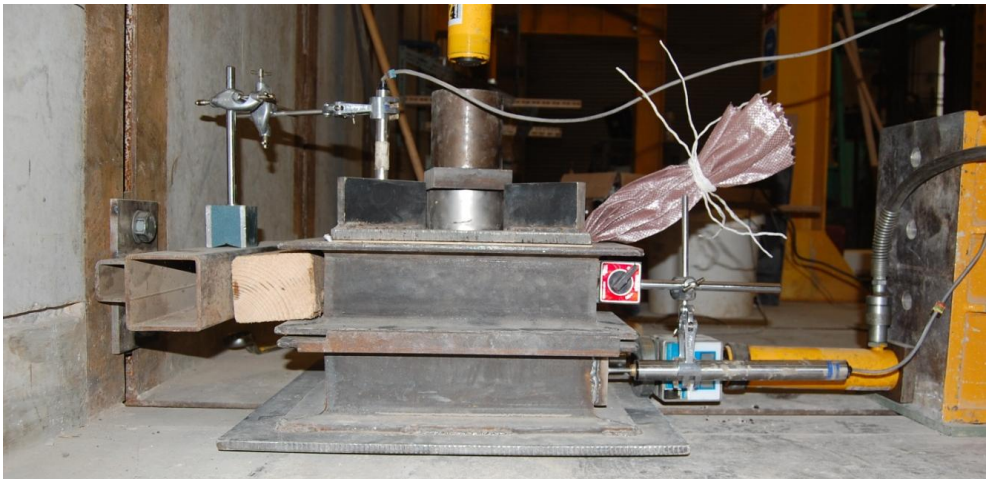

Figure 4.3: Earthbag shearbox test setup.

The test was set up as shown in Figure 4.3, with a constant normal load applied to each sample, and shear displacement applied by means of a 5T hydraulic jack operated by hand pump. The direction of shear was longitudinal with respect to the bags, parallel to the barbed wire strands. Normal and shear forces and displacements were measured at a rate of 10 readings per second.

18 shearbox tests were carried out on polypropylene bags in this programme. Tests on bag interfaces without barbed wire were repeated 3 times and carried out with applied normal loads of 2kN, 7kN, 12kN and 17kN. The following tests were also carried out on bag interfaces with two longitudinal strands of four-pointed barbed wire: 1 test at 2kN normal load, 3 tests at 7kN normal load, 1 test at 12kN normal load. An additional test on a bag and barbed wire interface, with the shearbox rotated 90 degrees to the direction of shear, in order to establish whether the direction of shear was significant. This test was also carried out with an applied normal force of 12kN.

4.3.1 Results

It was found that the peak shear strength of the bag interfaces was reached after a period of mobilisation, and then remained constant over large values of shear displacement. Table 4.3 shows the results obtained from the earthbag shearbox tests, including displacement to full mobilisation. As the actual applied normal load varied slightly with time, the values of average normalised shear force were obtained by taking a large number of data points and multiplying by the proportion of actual normal force to desired normal force:

$$\sum^{n} \frac{1}{n} \times shear\ force \times \frac{actual\ normal\ force}{desired\ normal\ force} \tag{4.1}$$

These values, shown in Table 4.3, were used in Figure 4.4 to find the friction coefficient and adhesion of the interfaces, indicated in Table 4.4.

Table 4.3: Earthbag shearbox test results.

	Normal force (kN)	Average normalised shear force (kN)				Mobilisation (mm)
		Repeat 1	Repeat 2	Repeat 3	Average	
No barbed wire	2	1.13	0.91	1.21	1.08	1
	7	3.19	2.94	2.93	3.02	1
	12	5.51	5.03	5.35	5.30	2
	17	7.22	7.31	7.40	7.31	2
Barbed wire	2	1.85	-	-	1.85	20
	7	3.64	4.97	7.00	5.20	5-20
	12	8.47	-	-	8.47	20
Barbed wire (transverse shear)	12	8.82	-	-	8.82	20

Table 4.3 shows good repeatability for tests on earthbag interfaces without barbed wire, but much poorer repeatability for those with barbed wire. This is most likely due to the inevitable variability that barbed wire will bring to the bag interface. The displacement to full mobilisation is also much greater for barbed wire interfaces. The behaviour of barbed wire in the interface between earthbags is considered in greater detail by Vadgama (2010).

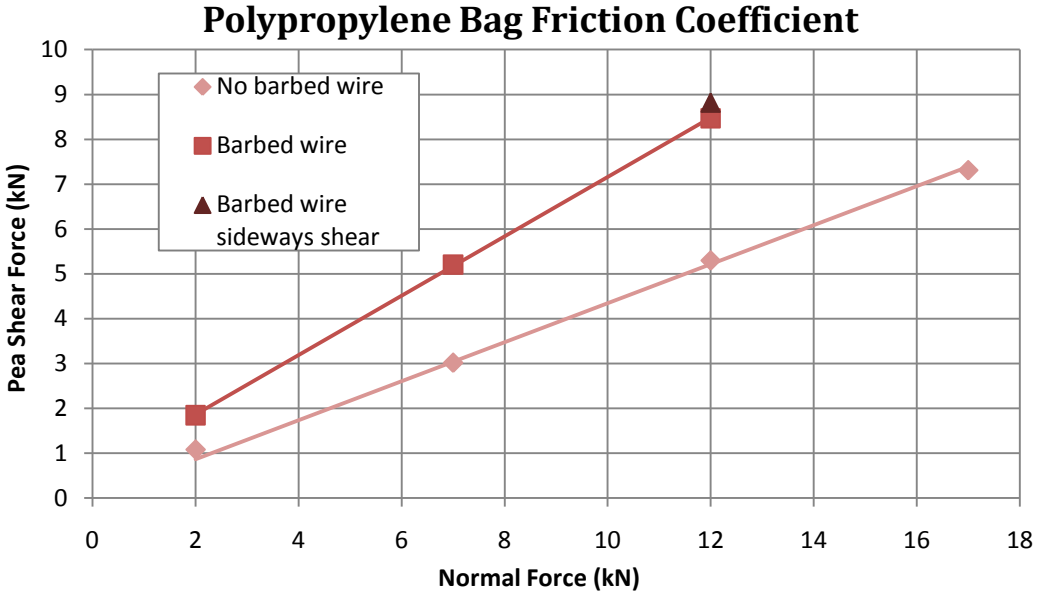

Figure 4.4: Graph showing shear force against normal force for bag interfaces.

Figure 4.4 shows the linear relationship of applied normal force against peak shear force for tested samples. The gradient of the trend line is the friction coefficient, and the y-intercept is the adhesion, both shown in Table 4.4. The samples without barbed wire have no adhesion, so the trend line was forced through the origin. Earthbag interfaces without barbed wire were found to have a friction coefficient of 0.43, and interfaces with barbed wire were found to have a friction coefficient of 0.66 and 8.15kN/m^2 adhesion. The graph shows that direction of shear appears to be independent of shear strength for barbed wire interfaces.

Table 4.4: Friction coefficient of polypropylene bag interface.

Sample	Friction Coefficient	Adhesion (kN/m^2)
No barbed wire	0.43	0
Barbed wire	0.66	8.15

Earthbag structural behaviour:

The material properties determined in Chapter 4 can contribute to the prediction of the structural performance of an earthbag system. Two sets of test were carried out in order to characterise their behaviour: Unconfined compression tests of bag stacks of varying height, and point-loaded arch tests. Both tests were carried out on stabilised and unstabilised earthbags. These tests will provide an understanding of the ultimate compressive strength of an earthbag wall, and the stability of an earthbag structure.

5 Compression Tests

A soil under vertical load exerts a horizontal pressure. If there is no force to resist this pressure, the soil will fall into a mound with sides sloping at the angle of the soil's internal angle of friction. In an earthbag, this horizontal pressure is resisted by the bag material, which confines the soil, keeping it in shape and giving the overall unit strength. Compression tests on bag stacks, such as those carried out by Daigle (2008) and Xu *et al* (2008), allow the compressive strength of the earthbags to be determined. Theoretically quantifying the compressive strength of an earthbag was a task considered by Xu *et al*:

5.1 Theory

5.1.1 Xu *et al*

Xu *et al* (2008) considered that in an unconfined compression test such as those they carried out, the stress experienced by the soil particles is due to the sum of the externally applied stresses and the stresses induced by tension in the bag material:

$$\text{Total vertical stress, } \sigma_y = \sigma_{y,ex} + \sigma_{y,t} \tag{5.1}$$

$$\text{Total horizontal stress, } \sigma_x = \sigma_{x,ex} + \sigma_{x,t} \tag{5.2}$$

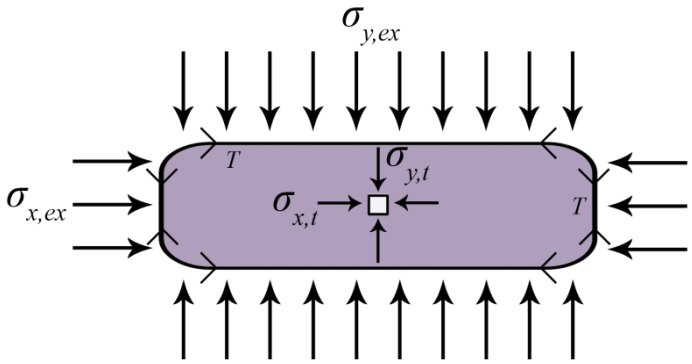

Figure 5.1: Bag cross section showing stresses acting on bag and soil particles.

The test is unconfined, therefore; $\sigma_{x,ex} = 0$. The stress due to the tension force in the bag material can be determined by examining a bag in cross-section (see Figure 5.1):

$$\sigma_{y,t} = \frac{2T}{B} \tag{5.3}$$

$$\sigma_{x,t} = \frac{2T}{H} \tag{5.4}$$

The loading plate moving against the soilbag mobilizes passive pressure in the soil, causing σ_y to increase until a state of plastic equilibrium is reached. Under these conditions, the vertical stress is the major principal stress, and the horizontal the minor principal stress. The relationship between principal stresses at this point, representing the maximum inherent resistance of the soil to lateral compression, can be written (Craig, 2004):

$$\sigma_1 = K_p \sigma_3 + 2c\sqrt{K_p} \tag{5.5}$$

Where:

$$K_p = \frac{1 + \sin\varphi}{1 - \sin\varphi} \tag{5.6}$$

Considering a soil particle of sand or gravel with no cohesion, equation (5.5) becomes:

$$\sigma_y = K_p \sigma_x \tag{5.7}$$

$$\therefore\ \sigma_{y,ex} + \sigma_{y,t} = K_p \sigma_{x,t} \tag{5.8}$$

$$\therefore\ \sigma_{y,ex} = \frac{2T}{H} K_p - \frac{2T}{B} \tag{5.9}$$

Now considering the soilbag itself as the particle, the externally applied stresses become the only stresses to consider, and we have established there is no external horizontal stress, therefore equation (5.9) becomes:

$$\begin{aligned} \sigma_{y,ex} &= K_p \sigma_{x,ex} + 2c\sqrt{K_p} \\ &= 2c\sqrt{K_p} \end{aligned} \tag{5.10}$$

By substituting these two equations, the apparent cohesion of the soilbag can be found, as shown in equation (5.12). From this the authors conclude that a frictional material can be considered as a cohesive-frictional material simply by wrapping it up with a bag (Xu et al, 2007).

$$2c\sqrt{K_p} = \frac{2T}{H} K_p - \frac{2T}{B} \tag{5.11}$$

$$c = \frac{T}{\sqrt{K_p}} \left(\frac{K_p}{H} - \frac{1}{B} \right) \tag{5.12}$$

Equation (5.10) gives the applied vertical stress, which when multiplied by the bag area at failure, gives a prediction of the compression strength of the earthbag. This analysis goes a long way to describing the behaviour of an earthbag under vertical compression, and the results obtained by Xu *et al* (2008) had only slight variation to the experimental results, which they assigned to inevitable inaccuracies in earthbag measurement.

In order for the tension force in the bag material to be uniform around its entire perimeter, the friction force between the bag material and fill material must be zero. This assumption is necessary for the simplicity of the model to be retained, but in reality of course, this friction will restrain the bag, which under vertical deformation will cause the top and bottom surface of the bag to experience greater tension, and the sides of the bag to experience less. It may therefore be inaccurate to consider vertical tension of the bag material. The noted irregularity of the earthbag dimensions could also alter particularly the vertical component of tension.

The above analysis also neglects friction between the soilbag and the loading plates. Transfer of tension from the bag material into the loading plate via friction could allow greater compressive forces to be resisted. It is unclear how this disparity was addressed during the experiments.

5.1.2 Infinite Stack Height Analysis

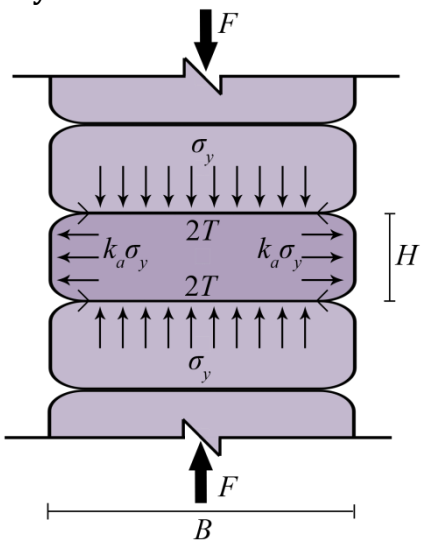

Figure 5.2: Infinite stack height analysis.

A simplification of this analysis can be achieved by considering an earthbag stack of infinite height shown in Figure 5.2, which therefore neglects the loading plates. Ignoring the self-weight of the bags, (which in a real stack is insignificant in comparison to the applied force) the applied vertical load, *F*, which fully mobilises the soil within the bags, generates a vertical stress of σ_y and a horizontal stress of $k_a\sigma_y$. The confining force is met by the bag material, such that:

$$K_a\sigma_y = \frac{2T}{H} \tag{5.13}$$

Where:

$$K_a = \frac{1-\sin\varphi}{1+\sin\varphi} \tag{5.14}$$

Equation (5.13) considers unit length of bag, similarly to the analysis of Xu *et al* (2008), and equates the horizontal compression of the soil to the tension of the bag material, per bag height, H. Considering the bag length, *L*, and width, *B*, we can then use the tensile strength of the bag material found in Chapter 4 to predict the ultimate failure load of the stack:

$$F = \frac{2T}{K_a H}\cdot LB \tag{5.15}$$

5.1.3 Bag Geometry at Failure

Both preceding methods of analysis are clearly highly dependent on the bag geometry at failure, and since large deflections are expected to occur before ultimate failure is reach, this geometry must be defined. Since tearing of the bag material is predicted to occur longitudinally on the top and bottom bag faces, it follows that at failure load, the horizontal bag material will have deformed to the strain at failure determined in the tensile tests in Chapter 4. Considering plane strain conditions, and constant volume of the earthbags, the geometry at failure can then be determined using bag dimensions found in Chapter 3.2:

$$B_f = B\left(1+\varepsilon_f\right) = 0.26\text{m} \tag{5.16}$$

$$L_f = L = 0.45\text{m} \tag{5.17}$$

$$H_f = H\cdot\frac{B}{B_f} = 0.093\text{m} \tag{5.18}$$

Alternatively, the experimental results for lateral deflections can be used to calculate the failure geometry of the bags. This method allows for consideration of deformations in three dimensions, but relies on experimental information and is therefore semi-empirical.

5.1.4 Predictions

Table 5.1 shows the predicted failure loads from each of the previously discussed methods of analysing an earthbag stack under vertical compression. The values for bag dimensions calculated above are used, along with the angle of friction of the fill material determined in Chapter 4.1.

Xu *et al*'s (2008) analysis is more conservative than the Infinite stack height analysis, as it takes into account the component of vertical stress imparted on the fill material by the tension in the bag. It is the justification of the latter method that due to the friction between the bag and fill materials, the settlement of the fill with increasing applied load, and the irregular geometry of the bags, this force is unlikely to occur in reality.

Table 5.1: Predicted earthbag compressive strength.

Analysis method	Ultimate failure load (kN)	Failure Stress (N/mm^2)	Failure strain (%)
Xu et al	103.8	0.89	11.4
Infinite stack height	134.0	1.15	11.4

5.2 Method

5 compression tests were carried out on a Dartec 200T testing frame, using the polypropylene bags and fill material described in Chapter 3.2. Bags were filled with 20kg of sand and tests were conducted on stack heights of 1, 3, 5 and 8. An 8-bag stack was also tested with stabilised fill material.

5.2.1 Sample Preparation

Bags were filled, and placed on the testing rig with their open end twisted and folded underneath the bag (see Figure 5.3). Daigle (2008) noted that although this is the way bag ends are treated in earthbag structures, the lack of adjoining bags could cause the ends to come loose and material to fall out. However, it was found that the friction due to the applied loads was more than sufficient to keep the bags tied securely and in place.

Figure 5.3: Earthbag on testing rig before and after tamping.

The bags were then tamped in place with a large, 20kg steel tamper, becoming block shaped and firm to touch, as shown in Figure 5.3. Each bag was tamped until the upper surface was relatively flat and level, the bag was no longer deforming visibly from further tamping, and the noise of impact changed from a dull thud to a 'ring'. This in practice equated to approximately 20-30 tamps, and constituted a noticeable change in the appearance of the earthbags, after which they were very firm to the touch and would even retain their solidity and form when lifted by hand.

For the 3 and 5 bag stack tests, two rows of four-pointed barbed wire were placed at the interface between bags, similarly to the earthbag shearbox test described in Chapter 4.3. The addition of barbed wire was in order to most closely replicate real project conditions. However, they were omitted for the 8-bag stack tests, because it was realised that the high magnitude of vertical load applied would be unlikely to occur in an earthbag structure, and the greater concern was to eliminate variables from the test.

Figure 5.4: 8-bag earthbag stack, with displacement transducer locations indicated.

Four percent cement was added to the fill material for the stabilised 8-bag stack test. No water was added to the fill; the moisture content of the soil was sufficient to set the material. The bags were left to harden for 21 days, and were then stacked on the testing frame. They were therefore not tamped in place, like the other samples.

5.2.2 Test Procedure

The vertical displacement was logged at one second intervals along with the vertical load. Testing proceeded at 5mm displacement per minute for the single bag tests, and 10mm/min for 3 and 5-bag stacks, 15mm/min for 8-bag stacks.

In the case of the 8-bag stack test, lateral displacements were also measured. Displacement transducers, indicated in Figure 5.4 were placed to measure horizontal deformation on one side and one end of bag 4, and on one side of bag 1. Transducers were located on a wooden tab attached to each relevant point, in order to account for the large vertical deformations expected.

5.3 Results

Figure 5.5 to Figure 5.7 show the plotted results for the 5 compression tests carried out on stacks of sand-filled polypropylene bags. As expected, large displacements were observed of up to 50% strain by test completion. In general, load increased non-linearly with vertical displacement until tearing of the bag material occurred. Upon initial tearing, the load capacity decreased and failure was defined.

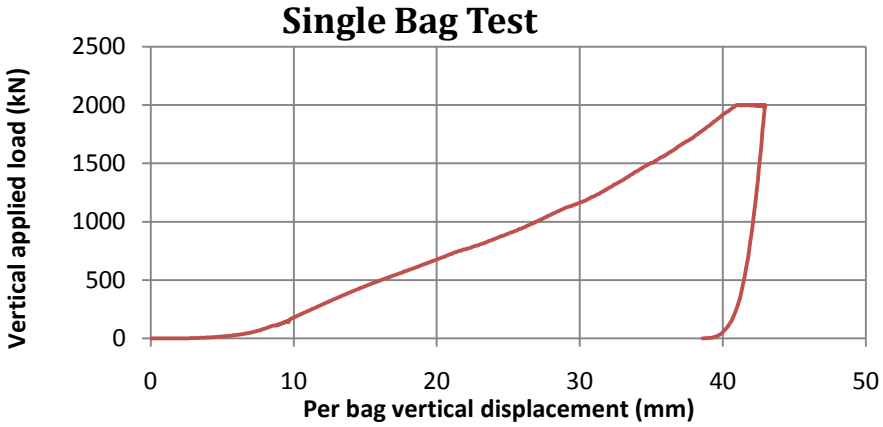

Figure 5.5: Force against vertical displacement for single bag compression test.

The single bag stack, plotted in Figure 5.5, did not achieve tearing failure. Instead the applied load increased until exceeding the capacity of the testing rig at approximately 40% strain. This was due to the low height-to-width ratio of the stack, and significant conclusions cannot be drawn from this test.

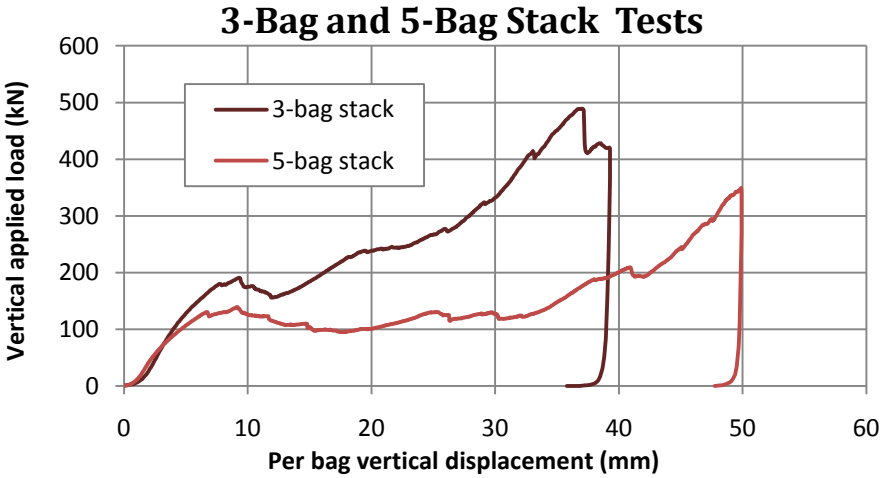

Figure 5.6: Force-displacement per bag response of 3-bag and 5-bag stack compression tests.

The compression tests of 3-bag and 5-bag stacks were continued significantly further than tearing failure of the bags to observe post-failure behaviour, as shown in Figure 5.6. Upon initial bag tearing, load capacity was slightly reduced. With further displacement, bag tearing continued and applied load peaked slightly higher than failure load. After further deformation which was largely plastic, bag tears were large enough that substantial portions of fill material began to fall out of the specimens. The 5-bag stack deformed plastically a substantial amount, until both test specimens underwent a renewed increase in load capacity due to the decreasing ratio of stack height-to-width.

Figure 5.6 shows that 3-bag and 5-bag stacks failed upon initial bag material tearing at similar values of applied load and per bag displacement of approximately 8mm. It was this behaviour up to failure that was focused on for 8-bag stack compression tests.

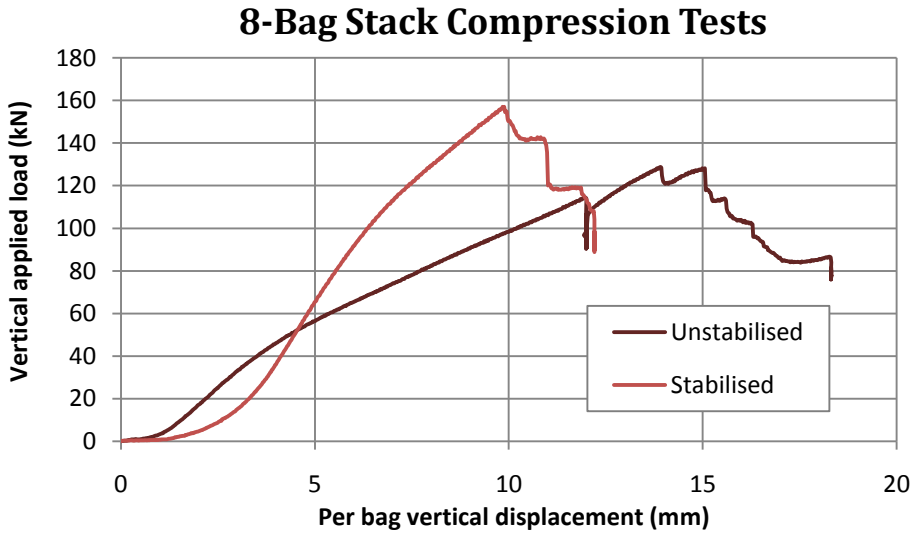

Figure 5.7: Stabilised and unstabilised 8-bag stack compression tests.

The load-displacement behaviour up to bag failure of the stabilised and unstabilised 8-bag stack compression tests is shown in Figure 5.7. The unstabilised test was paused for a short period at 12mm per bag displacement, which caused a small load drop off that was mostly recovered upon continuation of the test. The figures compared in Table 5.2 show that the stabilised stack achieved a 37% higher failure load, at a lower value of per bag displacement. The load drop-off of the stabilised stack was more considerable and immediate.

The load-displacement response of the sandbag stacks was similar in all cases: Stiffness started very low, as the irregular shape of the sandbags came into contact with the upper loading plate. Stiffness then increased as the sandbags conformed to the applied load; the contact area between bags increased as the interfaces flattened and the bag material straightened. Upon reaching peak load, bag tearing was heard within the specimen and the applied load decreased.

Figure 5.8: Bag tearing of unstabilised 8-bag stack compression test.

Among all of the tests where failure occurred, the initial bag tears formed longitudinally on the upper and lower faces of the earthbags. These tears occurred in all faces, except for those in contact with the loading plates, where friction with the stiff loading plate prevented tearing. Where barbed wire was included in the 3 and 5-bag stack tests, two parallel tears formed along the line of the barbed wire strands. In the 8-bag stack tests, where barbed wire was omitted, only one tear was present in each bag face, as shown in Figure 5.8.

5.3.1 Lateral Displacements

Lateral deformations of the 8-bag stacks were measured at certain points to record to changing bag area. The accuracy of the lateral displacement measurements was affected by the large vertical deformations, initial settling and rotating of the stacks. However, a linear relationship between vertical and lateral displacements was observed for the unstabilised stack up to the point of failure (see Figure 5.9). As mentioned, data from the transducer measuring displacement at the side of the middle back was disturbed by the overall rotations of the stack, therefore the lateral displacements were assumed to be uniform across all bags, and data from the bottom bag used instead.

Figure 5.9 shows that at bag failure of 11.9mm vertical per bag displacement for the unstabilised stack, lateral displacements were 7.1mm each side and 15.4mm each end. For the stabilised stack, Figure 5.10 shows lateral displacements of 5.7mm each side and 8.9mm each end. Displacement transducer locations are indicated in Figure 5.4.

Table 5.2: Compressive failure load of unconfined bag stacks.

Stack height (no. bags)	Failure load (kN)	Per bag displacement at failure (mm)	Failure Stress (N/mm^2)	Failure Strain (%)
3	190.70	9.3	-	8.9
5	130.34	6.7	-	6.4
8	114.33	11.9	0.97	11.3
8 (stabilised)	157.06	9.8	1.37	9.3

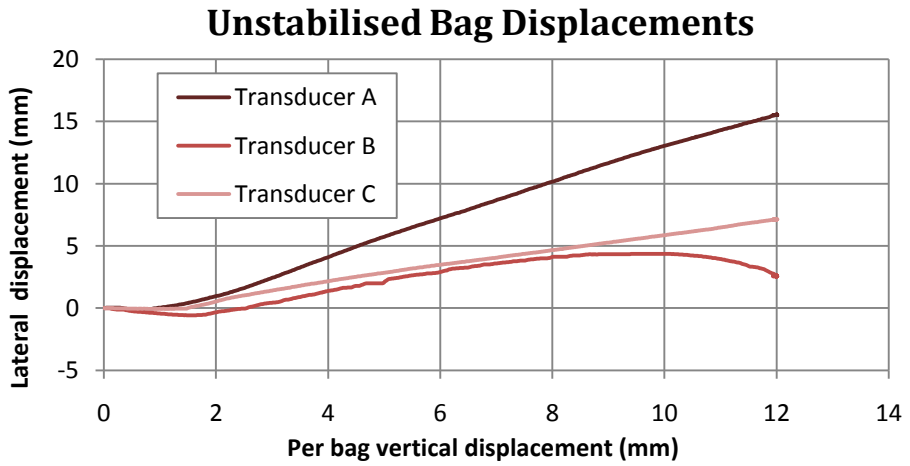

Figure 5.9: Graph showing lateral displacements of unstabilised 8-bag earthbag stack.

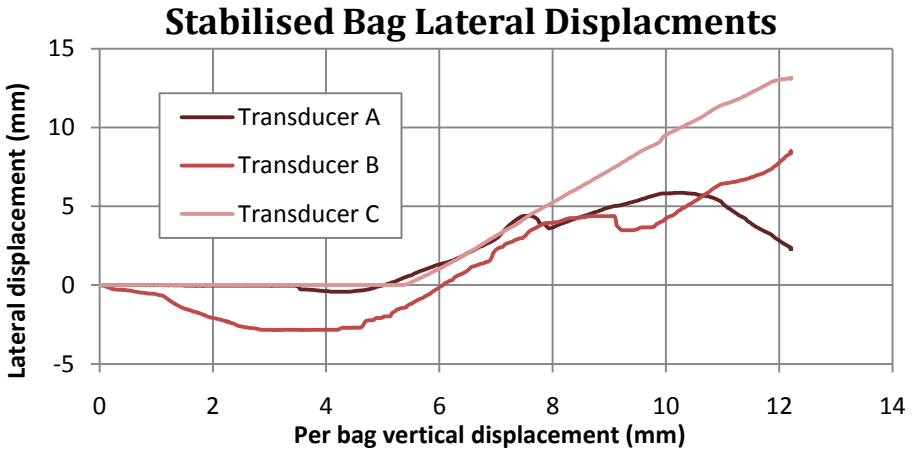

Figure 5.10: Graph showing lateral displacements of stabilised 8-bag earthbag stack.

5.4 Analysis

5.4.1 Effect of Increasing Stack Height

As has been observed by Daigle (2007), increasing the stack height decreases the compressive strength of the earthbag stack. This is due to the confinement caused by the loading plates having a lesser impact as the overall height of the stack increases. For this reason the 8-bag stack results are the most relevant, as they best represent the expected behaviour of a real earthbag structure.

5.4.2 Failure Mode

It can be observed in Figure 5.8 that the fill material has experienced relative vertical displacements across the bag tear line to the order of up to 5cm. This was the case for all earthbags in both stabilised and unstabilised 8-bag stack tests. Another notable observation is that the location of the tear line progressed diagonally across the bag faces throughout the height of the stack. These factors are indicative of a shear plane having formed in the earthbag stack, and this is the failure mode that has occurred for both 8-bag tests.

This finding helps to explain why the measured lateral deformations were larger than those calculated using a constant volume assumption of the earthbags. Due to tamping of the earthbags, the fill material was dense and therefore expanded during shear failure.

This shows that at ultimate limit state, earthbag structures could be considered as cohesive, dense soils.

5.4.3 Model Accuracy

As mentioned above, the results of the 8-bag tests are the most representative and will be used for comparison with theoretical predictions. The prediction of failure strains was not entirely accurate, but the impact on failure load is less than 10%, therefore will be ignored. A greater understanding of the failure mode of earthbags under compression has now been achieved, so future models could use knowledge of the density of the soil to better predict strains.

Table 5.3 shows that, for the unstabilised stack, Xu *et al*'s (2008) method is slightly over-conservative and therefore a more appropriate model to use than the under-conservative infinite stack height model devised earlier. No account was made for the effect of stabilisation on the strength of the earthbags, however. This could be addressed by considering the effective cohesion that the fill material gains from stabilisation, and adding this to the effective bag cohesion found in equation (5.12).

Table 5.3: Predicted and recorded values of compressive failure load (kN).

Theory		Experiment	
Xu et al	Infinite stack height	Unstabilised	Stabilised
103.8	134.0	114.33	157.06

6 Arch Tests

The most accurate and comprehensive way of gathering information on the behaviour of a structure is to build and test full-scale models of the entire structure. However, this is very rarely possible in practice, and the limitations of this investigation make two-dimensional tests more appropriate. Earthbag structures built using the flexible form rammed earth method invariably consist of one single or multiple intersecting domes. An arch could be considered as a two-dimensional representation of a dome. Although it lacks the structurally beneficial three-dimensional effects such as hoop stress, these effects are often ignored during design. Arches also occur as elements within earthbag structures, such as to span across door and window openings, and at the intersection of two domes. This makes the arch form highly appropriate for studying the behaviour of earthbag structures.

There are unfortunately no experimental precedents to draw information and experience from for these tests, so test conditions will be designed to replicate project conditions, particularly with respect to the Namibian project discussed in Chapter 3. Plastic theory will also be drawn upon to predict the behaviour of the arches.

6.1 Theory

Plastic limit state analysis was discussed in Chapter 2.5 as an analysis method often applied to masonry structures. In its simplest form, proposed by Heyman (1969), it makes an appropriate starting point for the analysis of earthbag structures for a number of reasons that will be explored here.

Firstly, a plastic method of analysis is appropriate for earthbag structures, because their behaviour will not be elastic and may be non-linear. Furthermore, Heyman's method does not rely on or consider any material properties other than density. This is convenient for a material such as earthbags where material properties are either unknown or variable. Lastly, the stresses expected in an earthbag structure are low in relation to the compressive strength of earthbags, therefore the assumption of infinite compressive strength is permissible, as compression failure of bags is unlikely to occur in an earthbag structure.

Depending on the failure modes found to dominate earthbag structures, the initial assumption made by Heyman of no sliding failure may also be permissible. However, if sliding failure is found to be significant, the plastic limit state analysis method can be further developed to take this into account.

The method also assumes that blocks are rigid. It has been shown in Chapter 5 that earthbags can undergo significant plastic deformations, even at low loads, therefore this assumption may not reflect the reality of earthbag structures. However, stabilised earthbags are stiffer and it may be found that deformations are small enough that geometry is unaffected.

6.1.1 Thrust Line Analysis

With the above assumptions in place, it is identified by Heyman (1982) that the analysis of a rigid block arch is a purely geometrical matter. Failure of the arch will occur by the formation of sufficient hinges to turn the structure into a mechanism. The challenge is to identify the locations of the hinges that will occur for the lowest possible load factor.

A simple program was developed to calculate the ultimate load required to achieve mechanism failure of the arches to be tested in this experimental programme. The values obtained will be compared to commercial software and actual results.

The program follows a number of steps to define the ultimate load in a purely geometrical manner, by calculating the possible location of the thrust line within the arch.

i) Define arch geometry:

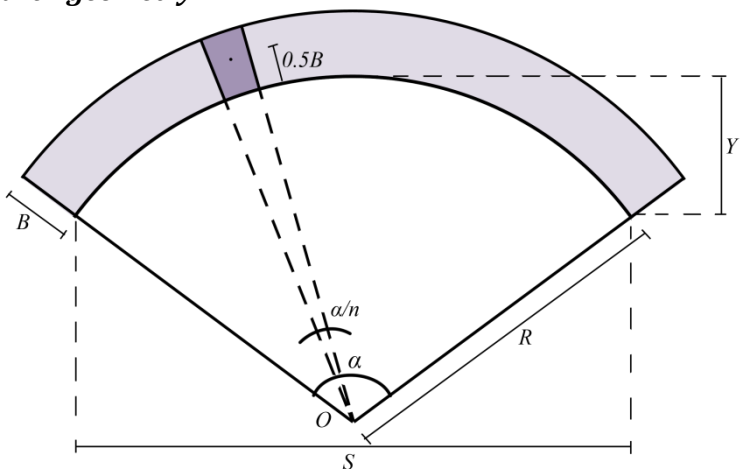

Figure 6.1: Segmental arch geometry.

Given a segmental arch of known span, *S*, and midspan rise, *Y*, the radius of curvature, *R*, and arc central angle, α, can be found from the equation of the circle (see Figure 6.1):

$$R = \frac{S^2}{2Y} + \frac{Y}{2} \tag{6.1}$$

$$\alpha = \sin^{-1}\frac{S}{R} \tag{6.2}$$

The arch is divided into n segments, each representing an earthbag and having a mass, *w*. The centre of mass of each segment is approximated mid-depth of the arch.

ii) Assign hinge locations:

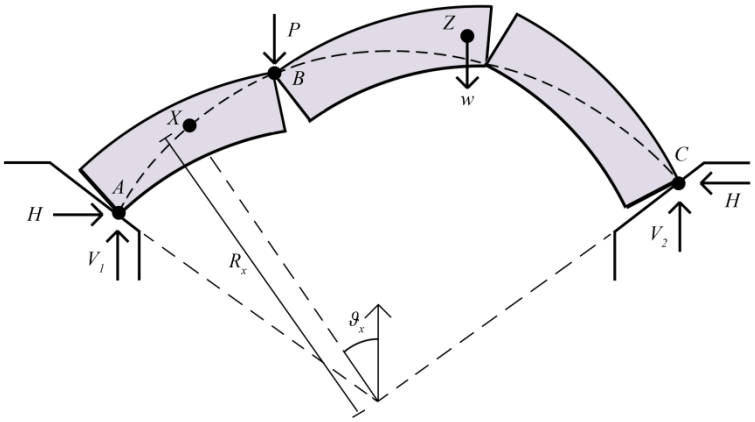

Figure 6.2: Arch four hinge mechanism.

The arch can be analysed as statically determinate once four hinges are defined along its arc. Each hinge occurs at the interface between segments at the intrados or extrados. For the case of the quarter span point load, engineering knowledge can be used to identify the location of 3 hinges, and the location of the fourth can be approximated and then iterated.

iii) Solve the simultaneous equations:

Four equations can now be set up to find the four unknowns: V_1, V_2, H and P. This can be done by creating free body diagrams that consider the arch clockwise of each of the hinge locations and taking moments about the origin for the three distinct cases. Vertical equilibrium forms the fourth equation.

iv) Find the location of the thrust line:

Moments can now be taken about the origin of free body diagrams at each bag interface, X, given in equation (6.3). This allows the location of the thrust line at each interface to be determined by the variable R_X, the radius to thrust line.

$$wR_Z \sum \delta_Z \sin\theta_Z = V_2(R_C \sin\theta_C - R_X \sin\theta_X) + H(R_C \cos\theta_C - R_X \cos\theta_X) + \delta_B P(R_X \sin\theta_X - R_B \sin\theta_B) \quad (6.3)$$

Where:

$$\delta_i = \begin{cases} 0, & \theta_i < \theta_X \\ 1, & \theta_i \geq \theta_X \end{cases} \quad (6.4)$$

v) Iterate the fourth hinge location:

The initially calculated thrust line may pass outside the width of the arch. The fourth hinge location can be moved to the location of maximum divergence of the thrust line outside the arch, and the calculations repeated until the thrust line runs entirely within the thickness of the arch.

This method of analysis has been developed into a spreadsheet in order to calculate predicted peak load of the arch experiments. The results from this spreadsheet can also be compared to a commercially available software package, Ring 2.0 (LimitState, 2009), which uses the same plastic limit state analysis method, and is also more powerful and customisable – able to include other failure modes than mechanism failure.

6.1.2 Predictions

Table 6.1: Predicted ultimate load of arch tests.

Analysis Method	Failure Mode	Ultimate Load			
		Arch 2	Arch 3	Arch 4	Arch 5
Thrust Line Analysis	Mechanism	11.18	LOCKED	11.18	11.18
Ring 2.0	Mechanism	14.34	LOCKED	14.34	14.34
	Sliding	8.01	41.77	8.01	13.73
	Crushing	11.02	39.5	11.18	11.02
	All 3	7.31	39.5	7.49	9.32

The predictions in Table 6.1 show that the thrust line analysis gives a lower value of failure load than Ring 2.0 for mechanism failure. These values correspond to the assumptions of infinite compressive strength and infinite friction. The thrust line analysis concludes that the arch is 'locked' under the condition of mid-span applied load. In practice, this means that when the load is applied at mid-span, straight lines can be drawn between the point of application of load and the abutments. This corresponds to an infinite load, and means that a mechanism failure mode would not occur for the particular load case.

The commercial software is able to develop the plastic limit state analysis method further by taking into consideration block crushing and sliding. Table 6.1 shows that for both quarter-span and mid-span applied load cases, sliding failure is the predicted critical failure mode. The effect of stabilising the fill material or introducing barbed wire to the bag interfaces can also be considered. Barbed wire increases the friction coefficient of the bag interfaces, which suggests block crushing will then become the critical failure mode. For the case of stabilising the fill material, the model predicts the ultimate load to cause crushing failure will increase, but that the critical failure will still be sliding failure.

The most significant assumption that this model relies on in relation to earthbag structures is that deformations of the blocks are insignificant and will not affect the overall geometry of the arch. In this respect, the model does not differentiate between unstabilised and stabilised arches. For this reason, these predictions are likely to be more accurate for the stabilised arch, where deformations will indeed be smaller.

6.2 Method

Five earthbag arches were constructed and tested in this experimental program:

Arch 1: Preliminary experiment to develop methodology. Arch loaded at quarter-span. Displacements not logged.
Arch 2: Unstabilised arch loaded at quarter-span.
Arch 3: Unstabilised arch loaded at mid-span.
Arch 4: Stabilised arch loaded at quarter-span.
Arch 5: Unstabilised arch loaded at quarter-span. Barbed wire included at bag interfaces.

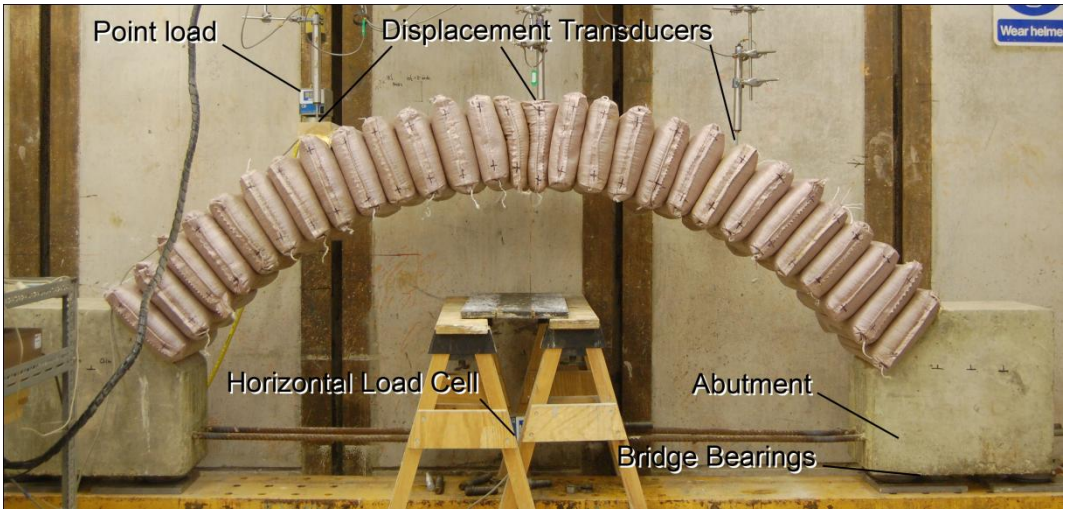

Figure 6.3: Setup of arch tests.

The arches were built on a plywood formwork which created an intrados with span length 2.2m and mid-span rise 0.5m. Concrete abutments were setup on bridge bearings to support the arches and transfer all lateral loads into a load cell between them which measured horizontal reactions. The vertical load was applied by means of a 5T hydraulic jack, with load cell attached to measure applied load. Displacement transducers were placed at mid-span and quarter-spans to measure vertical deflection of the arches (see Figure 6.3). The vertical load was applied across two bags to prevent an over-concentration of stresses occurring towards the applied load, which could result in severe local deformation of the bags. This spreading of the applied load is of the same order of magnitude of the area loaded by a person stood on the structure.

The first arch was built to verify and improve the test methodology. Since there are no precedents for earthbag arch tests, it was necessary to carry out a preliminary investigation into the feasibility of the test. The arch was loaded by point load at the quarter span until failure, but no displacements were recorded. As a result of this trial, the concrete abutments were separated by approximately 200mm in order to fit the earthbags more accurately, and initial tamping of the earthbags was carried out on the ground before placement within the arch.

6.2.1 Construction of the Arches

In the same way as during the 8-bag stack compression tests, earthbags were initially tamped on the ground, then placed into the arch and tamped into position. The initial tamping was carried out with a large metal tamper, and final tamping with a sledgehammer and a piece of timber to distribute the force of impact across the bag face. This method allowed the maximum tamping of the bags to be achieved, and ensured they ended up well positioned within the arch, with large areas of contact between each bag. In a real earthbag structure, the arch would be tamped from above and further earthbags would be placed onto the arch to form the roof of the structure. Keystones were given a more defined wedge shape during initial tamping so that they could be placed easily into the arch. They were then tamped from above to 'seal' the arch.

6.2.2 Application of Load

The vertical load was applied manually with a hydraulic hand pump, and force and displacement readings were measured at 1 second intervals. Photographs were also taken at intervals to observe the overall arch deformation. The load was removed at least twice during each test to record elastic recovery and permanent deflection. The loading jack was operated until total failure of the arch occurred.

6.3 Results

The load-deflection plot for each of the four displacement-measured arch tests is shown on the same set of axes in Figure A1 in Appendix A, allowing for visual comparison of the arch behaviours. Each of the four measured arches is discussed in turn, with Figure 6.5 to Figure 6.8 showing the individual load-deflection plot of each arch, characteristic photographs and a super-imposed plot relative arch displacements. The plots are generated directly from the photographs to give a clearer visual demonstration of the relative movements of the arches.

Table 6.2 shows the key values of applied load and displacement recorded from each of the four measured arch tests.

Table 6.2: Arch test results.

Arch	Peak load (kN)	Peak load displacement (mm)	Collapse displacement (mm)	Percentage recovery (%)
2	4.12	41.8	147.4	22.8
3	7.69	64.3	96.8	21.1
4	7.26	8.8	54.2	57.4
5	3.85	40.4	-**	26.7*

NOTE: *Value obtained from second unload cycle only.
**Large displacement. Could not be measured.

6.3.1 Arch 1

The lack of initial bag tamping on the ground before placement within the arch meant that the bags were less compact than for the other arch tests. The positioning of the abutments meant that the lower bags did not rest entirely on the abutments, as shown in Figure 6.4. This allowed hinges to form at the base of the arch in the middle of the earthbag rather than at the extrados, essentially halving the effective depth of the arch. This greatly decreased the load carrying capacity of the arch, which withstood an ultimate load of only 1.3kN.

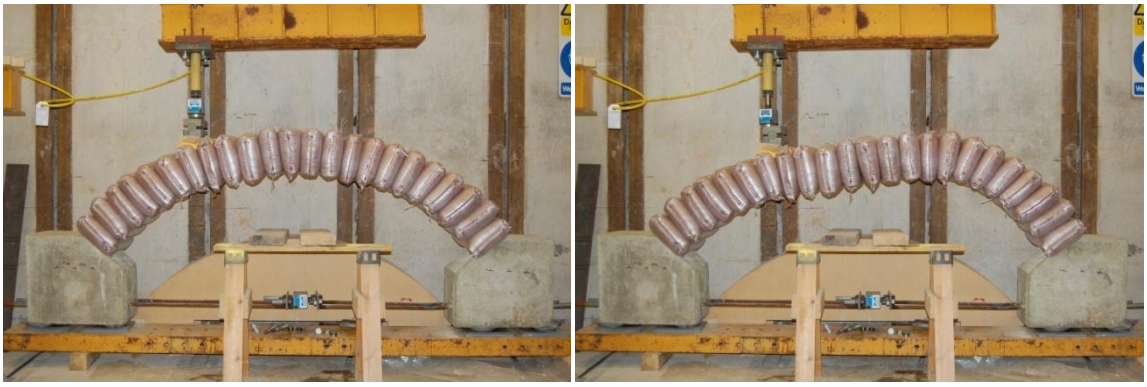

Figure 6.4: Arch 1 (left) before loading and (right) just before collapse.

6.3.2 Arch 2

As can be seen from comparing Figure 6.4 and Figure 6.5, the improved methodology employed during the construction of the second arch created a more uniform appearance and stronger looking arch. Initial tamping on the ground enabled more energy to be imparted into each bag, making the bag thickness smaller, meaning there were 5 more bags in Arch 2 than in Arch 1. The arch depth is also larger because of this increased tamping of the bags. Unlike the first arch, the full area of the bags at the springings are in contact with the abutments, greatly increasing the overall stability of the arch, and allowing the effective depth to extend the full depth of the arch. This method of constructing the arches was followed for the duration of the experimental programme.

The behaviour of Arch 2 can be loosely characterised into three distinct modes, which occur as the test progresses: Linear response, large deformation and sliding. Initially, the arch exhibits a linear load-deflection response, with relatively stiff behaviour and small displacements. Figure 6.5 shows that initial deformation of the arch is small and smoothly distributed along the length of the arch, similar to the behaviour that would be expected from a rigid block arch such as masonry. Towards reaching peak load, the plastic deformations of the arch begin to increase significantly. Once peak load is achieved, the load carrying capacity of the arch decreases, and continues to decrease, as large deformations and rotations of the bags destabilise the arch. This continues for large values of displacement, until the deformation of the arch has reduced the normal compression at certain bag interfaces sufficiently to allow significant sliding to occur between bags. The arch then collapses with a combination of sliding and rotation of bags.

Figure 6.5 shows the stiffness of the unloading/reloading cycle is consistent through the 3 cycles. 22.8% of the deformation is recovered each cycle, showing the predominantly plastic behaviour of the arch. There are, however, no visibly defined hinge locations during the large rotations and deformation of the arch. Instead, all of the bags rotate a small amount relative to each other, distributing the rotations throughout the arch. The left hand side of the arch, under the applied load, gradually rotates into a flat beam, pushing the right hand side of the arch up. Sliding then occurred at the interface with the keystone bag, with flattened ‘beam’ rotating about the left abutment.

6.3.3 Arch 3

The behaviour of the centrally loaded arch 3 followed a similar pattern, in that it began exhibiting a linear load-deflection response, and then became highly plastic, with large deformations and rotations occurring along the length of the arch. In particular, a similar beam developed, as shown in Figure 6.6, this time under the load in the middle half of the arch, pushing up both of the springings.

Due to the more structurally favourable location of the load, less displacement occurred for a given load, and higher peak strength was achieved. The relative plasticity of the arch was similar, with 21.1% of displacements being recovered upon unloading/reloading cycles.

The loading jack became fully extended during the test around 40mm central displacement, necessitating an unloading of the arch to insert a spacer under the load. This destabilised the arch due to the large deformations and rotations that had already occurred, and may have prevented a higher peak load from being achieved. The load was again removed at around 100mm central displacement, which caused the arch to collapse. This meant there was not an opportunity to observe the sliding failure seen in Arch 2.

6.3.4 Arch 4

The stabilised arch exhibited the most diverse behaviour of the four measured arches. The initial stiffness of arch 4 is much higher, and a significantly higher peak load was achieved, as is especially apparent in Figure A1. Similarly to Arch 2, there is initially a linear load-deflection response. The large plastic deformations did not occur in the same way. Instead, upon reaching peak load, the arch suddenly changes behaviour to a linear applied load inversely proportional to displacement. The load continued to decrease at a constant rate until collapse.

The stabilised arch recovered a much larger proportion of displacement upon unloading, at 57.4%. This demonstrates the increased elasticity of the stabilised arch. Also unlike the unstabilised arches, Arch 4 developed defined hinge locations, visible in Figure 6.7. The most defined hinges are under the applied load at the extrados, and at the opposite quarter span at the intrados. There are also significant rotations of the end bags about the abutments, but the hinges are not as apparent. It is possible that the rest of the rotation required to form the arch into a mechanism was distributed about a number of bag interfaces, with particularly large rotations at the base of the arch.

6.3.5 Arch 5

The variable explored with Arch 5 is the inclusion of barbed wire. The results can be seen from Figure 6.8 to be similar to the equivalent arch without barbed wire; Arch 2, with the barbed wire causing slight variations in the behaviour of the structure, that were not necessarily as expected.

The initial stiffness of the arch and the displacement recovery upon unloading are both similar, although the low overall displacement of the arch upon first unloading made the results unreliable, meaning there was only one unload/reload cycle to draw data from. However, a lower peak load was achieved by Arch 5, and at a slightly lower value of displacement. This suggests that the barbed wire did not improve the structural strength of the arch.

Figure A1 also suggests that Arch 2 sustained higher overall deformations and rotations before finally collapsing. This is in fact untrue – the deformations became so great towards the end of testing Arch 5, and the arch was so unstable that measurements of the displacements could no longer be made. The barbed wire seemingly contributed towards holding the arch together long after the other arches would have collapsed.

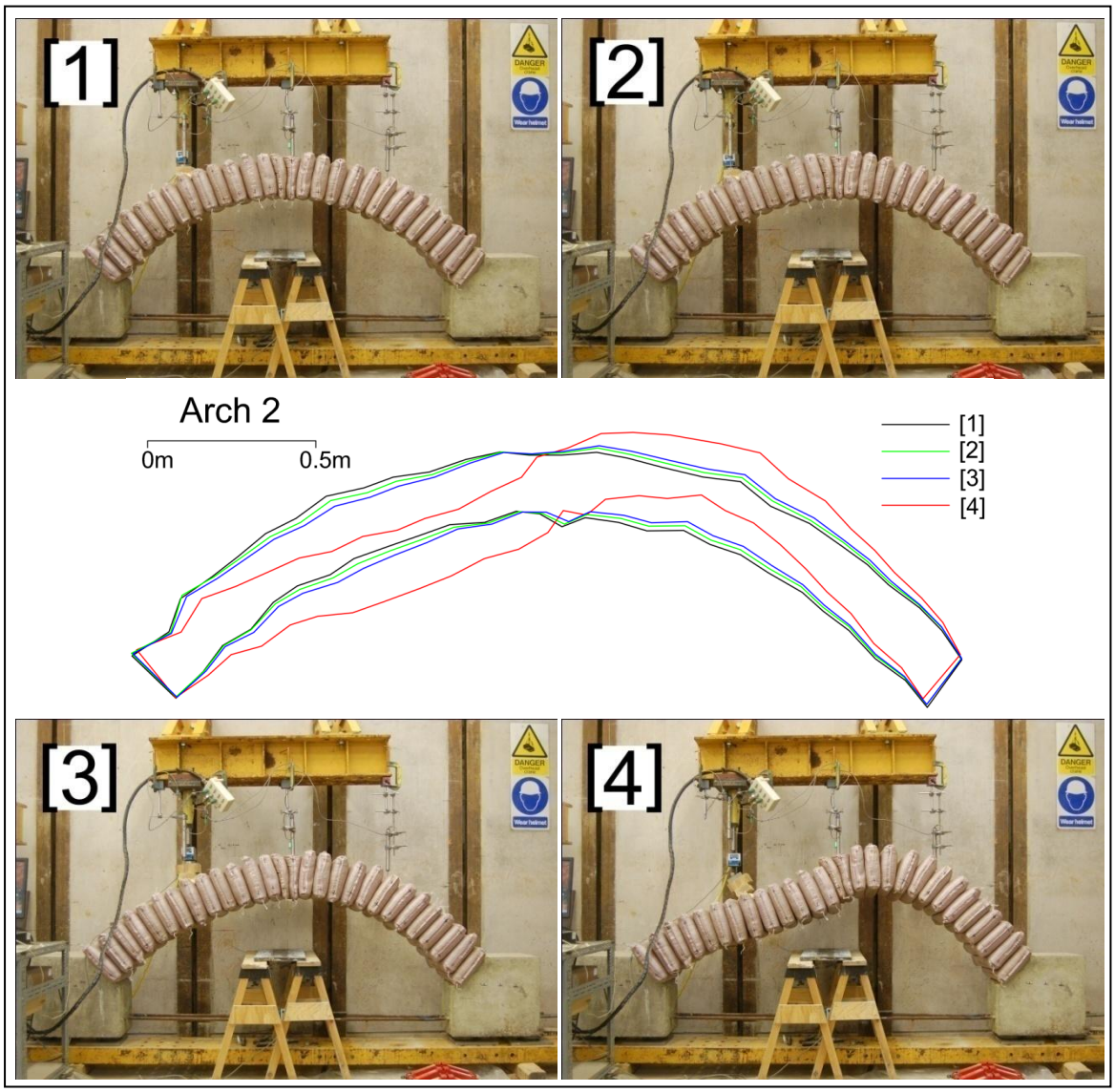

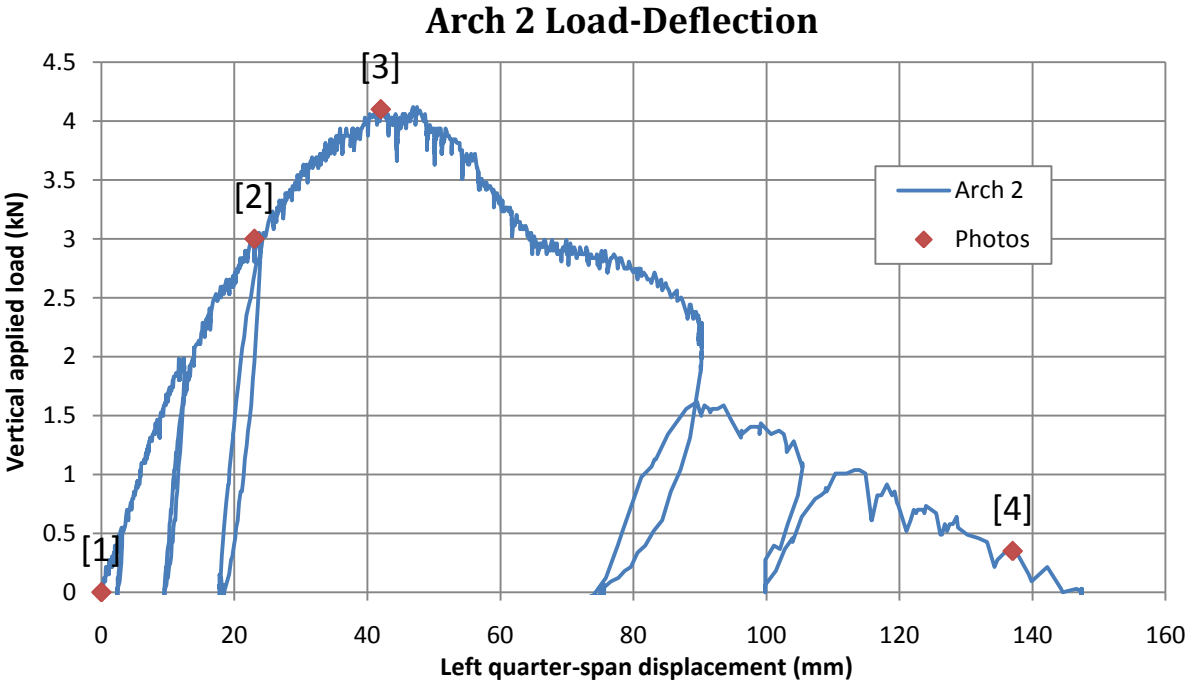

Figure 6.5: Load-displacement response of Arch 2, and numbered photographs.

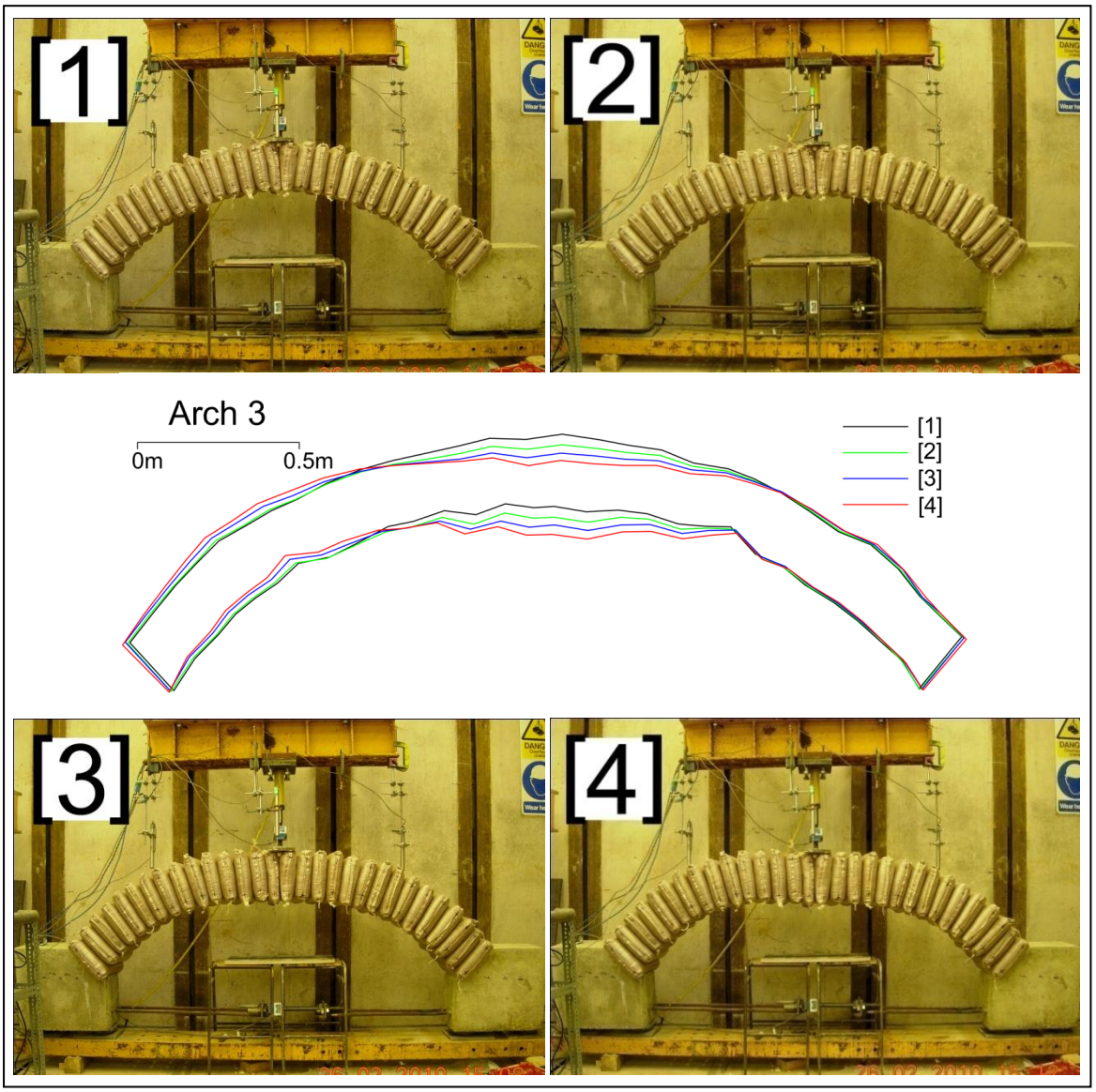

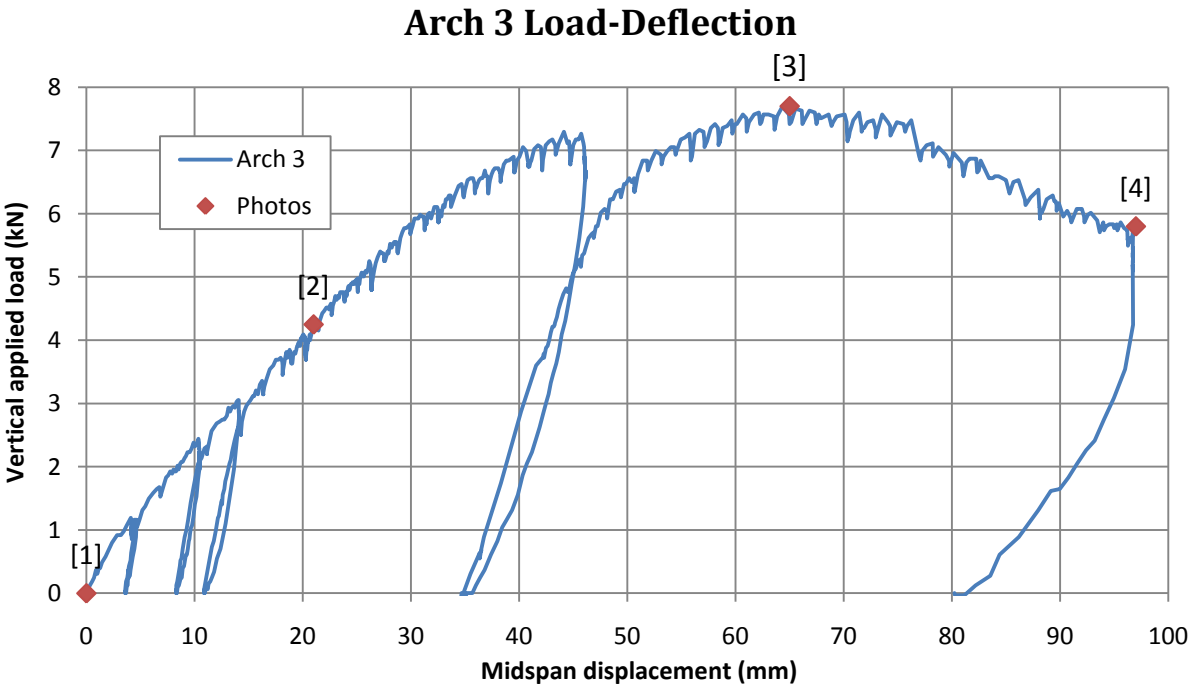

Figure 6.6: Load-displacement response of Arch 3, and numbered photographs.

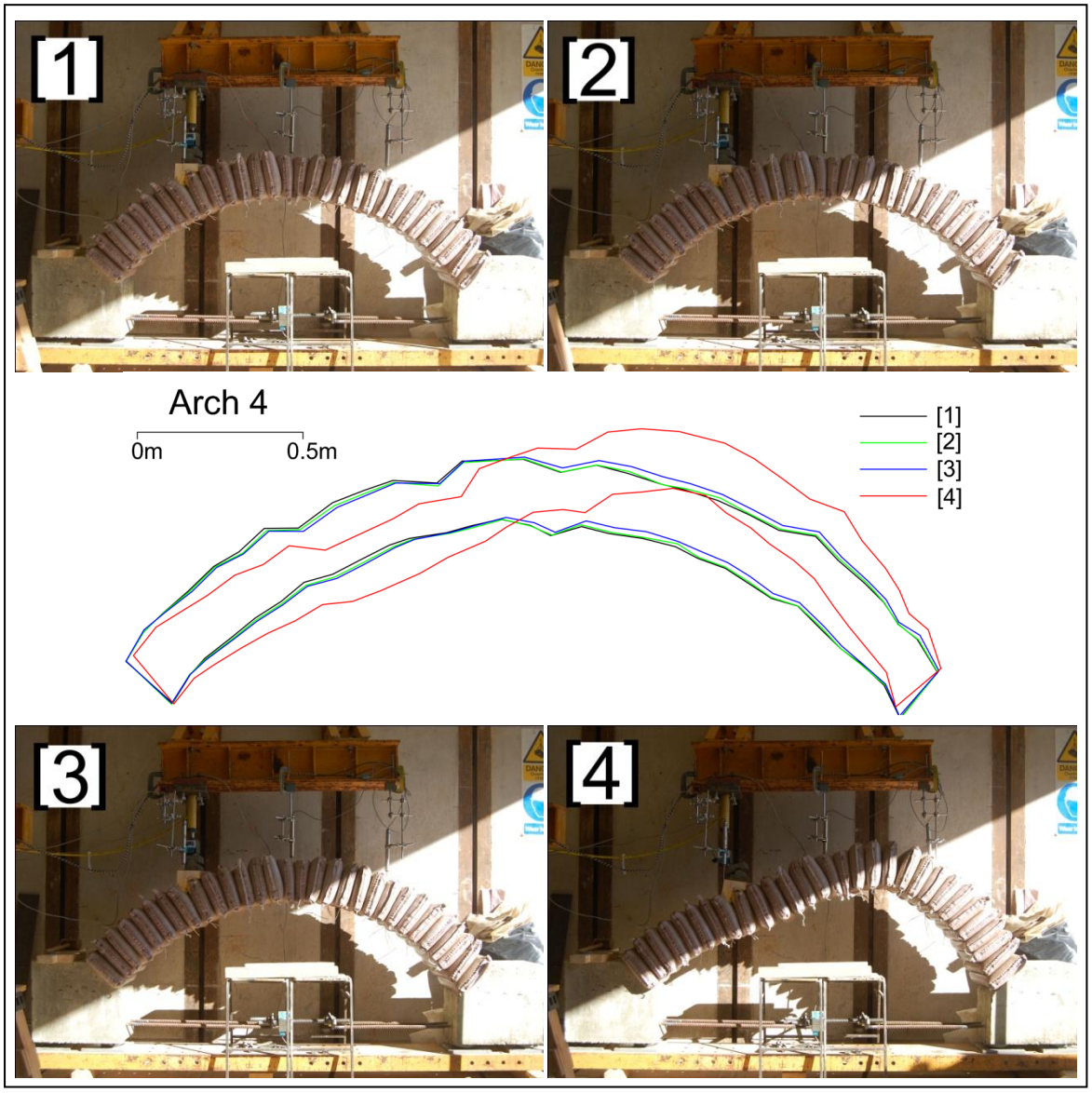

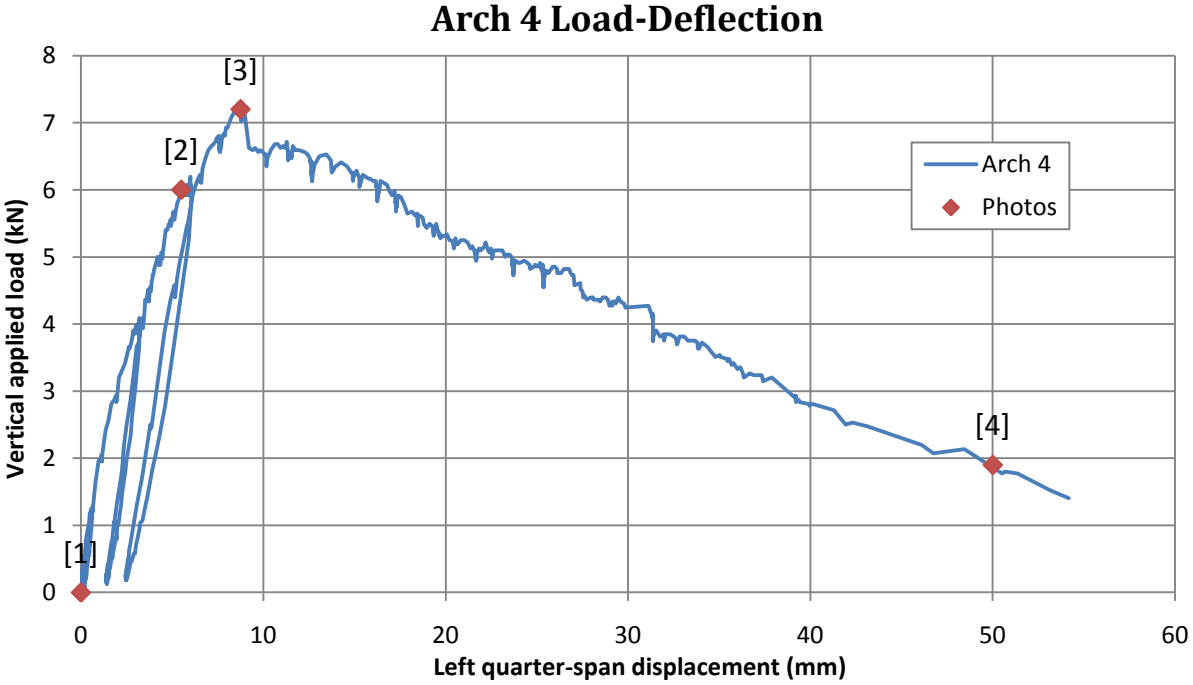

Figure 6.7: Load-displacement response of Arch 4, and numbered photographs.

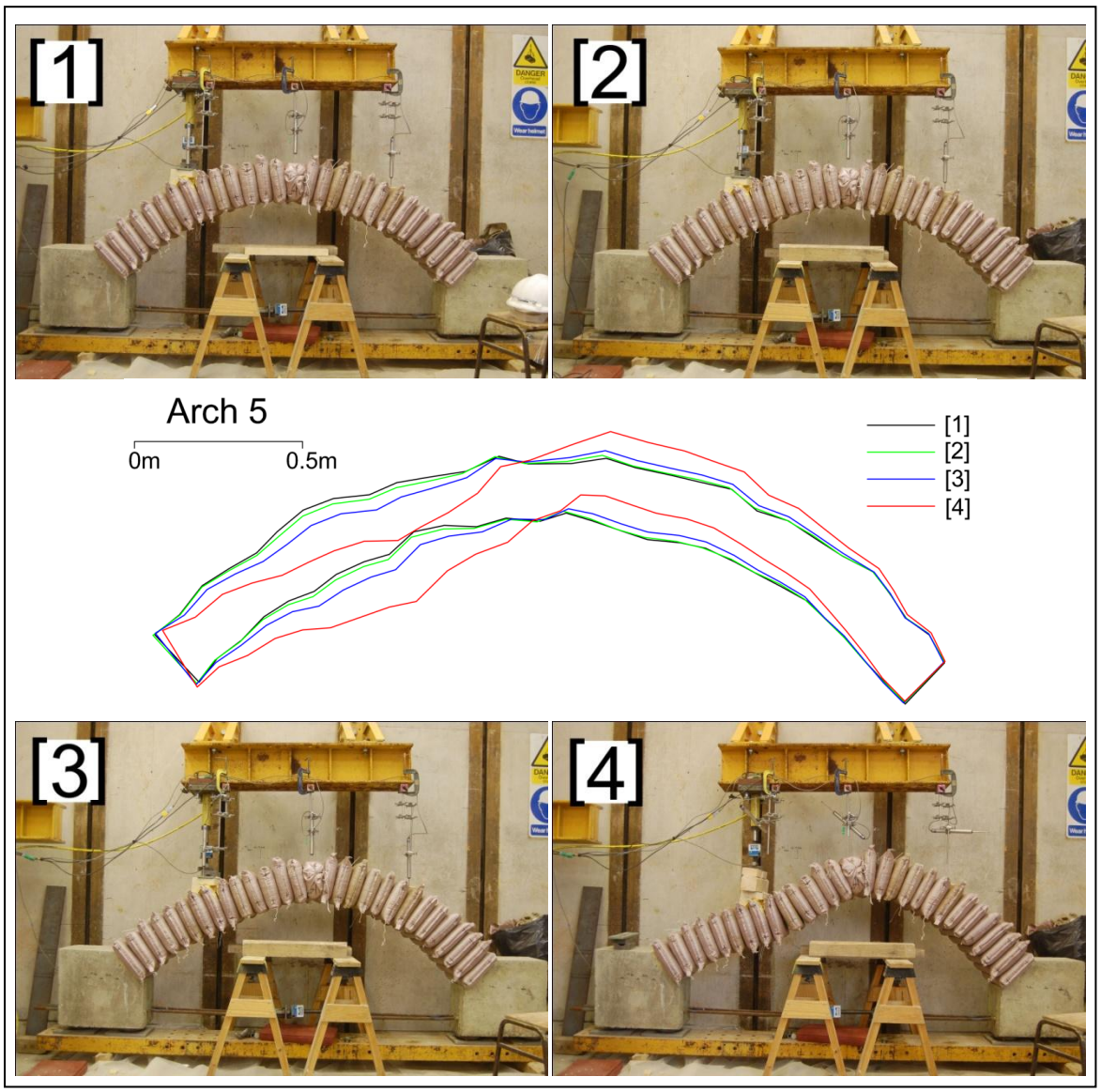

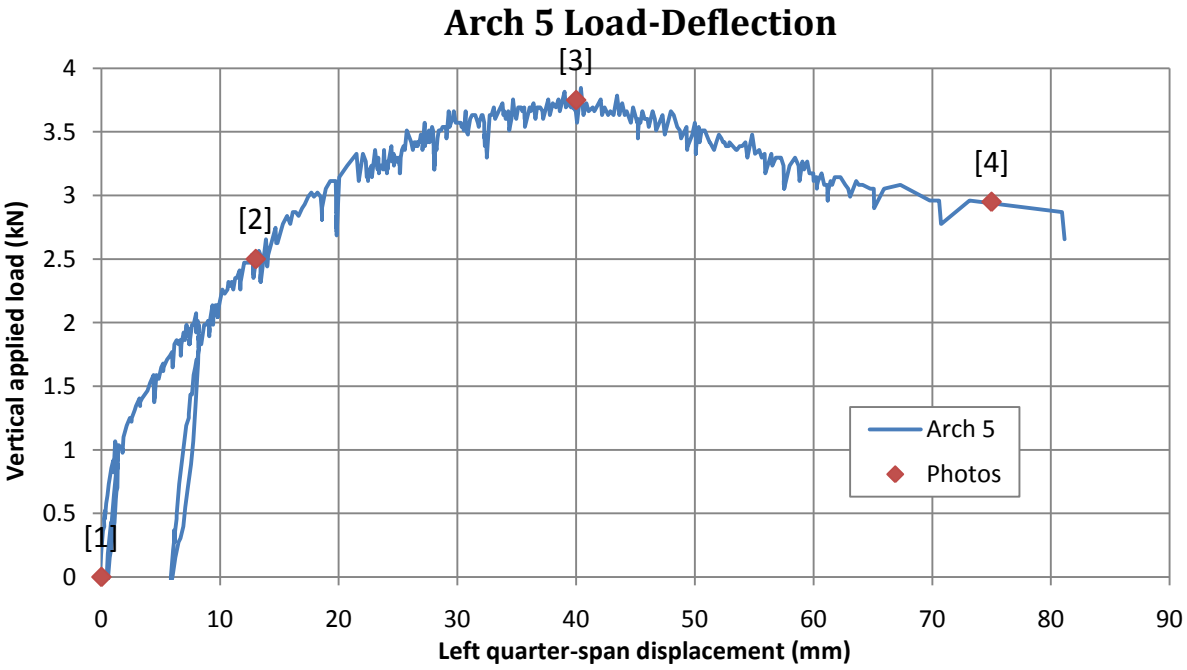

Figure 6.8: Load-displacement response of Arch 5, and numbered photographs.

6.4 Analysis

Comparison of the arch tests allows us to explore the impact of each tested variable on the behaviour of earthbag structures. Those variables considered are the location of applied point load, addition of barbed wire at the bag interfaces, and stabilisation of fill material. Comparison of experimental results with theoretical predictions allows examination of the model used to predict behaviour. Unfortunately, due to the lack of experimental precedent, comparisons cannot be made with similar earthbag structural tests.

Firstly, the overall similar behaviour of the arches can be noted. In all tests, the arches developed large deformations and rotations before collapsing. These deformations were predominantly plastic. Figure A1 shows the initial linear load-deflection response of the arches towards peak load, becoming more plastic until applied load decreases.

6.4.1 Failure Mode

Large deformations and rotations occurred before ultimate collapse of the arches. Sliding between bags was also noted in all tests leading up to collapse. Failure was therefore a combination of sliding and mechanism modes, as predicted by Ring 2.0. For structural purposes, the arches had become unstable long before final collapse occurred. This can be seen from the inability of Arches 2 and 3 to fully recover their load after undergoing an unload/reload cycle close to or beyond peak load, shown in Figure A1.

Considering serviceability limit state, the large deflections experienced mean this would be reached before peak load. For example, with render applied, a span/deflection ration of 180 permits 12.2mm deflection, which is exceeded long before peak load for all but the stabilised arch, Arch 4. For unstabilised earthbag structures, serviceability state is therefore likely to be the most critical case to consider.

6.4.2 Location of Applied Load

Although Arch 3 achieved a peak load 87% higher than that of Arch 2, this is not as great as the 432% increase predicted by Ring 2.0 analysis software. This suggests that factors other than those considered in the analysis also contributed towards the failure of the arches.

6.4.3 Stabilisation

The stabilised arch showed the most predominant variation in behaviour, achieving a 75% higher peak load than its equivalent unstabilised arch, with lower displacements and more linear behaviour, with greater recovery of displacements. This represents a significant structural improvement in performance, and demonstrates that the stabilisation of earthbag structures generates a markedly different behaviour.

This increased stiffness of the stabilised arch means that serviceability limit state will be less restrictive on the performance and may even be less critical than ultimate limit state. The linear load-deflection response of the arch right up to peak load also suggests the arch did not become destabilised in the same way as the unstabilised arches did.

Stabilising the fill material also has practical benefits for an earthbag structure, as if the fill material has sufficient structural strength of its own the structure is no longer vulnerable to UV decay of the polypropylene bags.

6.4.4 Barbed Wire

It was found that the addition of barbed wire did not increase the strength of the earthbag arch, but decreased the peak load by 6.5%. This result was not expected, but there are a number of possible explanations for this behaviour:

The number of tests conducted is low, and tests were not repeated. It is possible that this variation reflects inaccuracies in the repeatability of the tests rather than the inclusion of barbed wire. Repeatability of the experimental programme is discussed further in Chapter 7. Inserting barbed wire at each bag interface made the aligning of bags more difficult, and also acts to separate the bag faces slightly. This could have contributed to the lower strength achieved.

The barbed wire did help to hold the arch together at the end of the test, but this is less significant to real structures, as serviceability is the more critical limit state. Unfortunately, Arch 5 did not possess a higher initial stiffness, suggesting that barbed wire will not significantly improve the structural performance of an earthbag structure.

However, whilst preparing test specimens, difficulty was experienced when tamping small stacks of bags without barbed wire between them, as bags would move around and require regular realigning. Using barbed wire as a shear key in real earthbag structures may improve the buildability, especially during tamping. This may also be achieved by other means, such Long strands of barbed wire encircling an earthbag dome could also help contribute towards 3D effects such as hoop stress and improve the overall stability of a three dimensional structure.

6.4.5 Plastic Limit Analysis Model

The thrust line analysis discussed in Chapter 6.1 was not able to correctly model the behaviour of the arches. Due to the irregularity and complexity of earthbag structures, a more comprehensive method is required to model their behaviour.

The critical failure loads calculated by Ring 2.0 commercial arch analysis software are shown in comparison with the experimental results for peak load in Table 6.3. The critical failure load predicted by the software was always that which considered mechanism, sliding and crushing failure (except for Arch 3 which was crushing and mechanism only). This largely agrees with the observed failure modes. However, the table clearly shows that there is very poor correlation between predicted and observed results for all unstabilised arch tests. The experimental results are all significantly lower than the predictions.

However, the predicted value of failure load for Arch 4, the stabilised quarter-span point loaded arch, is accurate to within 5%. This is a positive result which, although only providing a sample of 1, gives an indication that the ultimate plastic limit state analysis method used could be appropriately applied to stabilised earthbag structures.

Table 6.3: Theoretical and experimental values of peak load.

Arch	Theory (kN)	Experiment (kN)
2	7.31	4.12
3	39.5	7.69
4	7.49	7.26
5	9.32	3.85

It was noted in Chapter 6.3 that the observed behaviour of the stabilised arch was markedly different from the behaviour of all the other arches. Therefore it is reasonable that the plasticity model should only fit one of the two observed behaviours. The crucial factor that makes the model more relevant to stabilised earthbag structures is because their behaviour more closely matches the assumptions made in the analysis:

6.4.6 Validity of Assumptions

It was discussed in Chapter 2.5 that plastic limit analysis was developed initially for steel structures, and then applied to masonry initially by Heyman (1982). In applying this method to a new material, we should now consider the validity of the assumptions associated with it:

- **Zero tensile strength:** This assumption is invariably true of earthbag structures, even more so than for masonry.
- **Blocks are rigid and deformations are small:** It has been found that this is an inappropriate assumption to make for unstabilised earthbags, even at low levels of stress, as deformations are large and bags deform significantly. The compression tests in Chapter 5 showed that deformation particularly occurs upon initial loading, when the earthbags have lower stiffness. However, it could be considered that, when stabilised, earthbags behave stiffer and exhibit a linear load-deflection response up to peak load. This is similar to the behaviour exhibited by masonry, and could be sufficient to consider this assumption adequate for loads not exceeding peak load x a factor of safety.
- **Friction between blocks is infinite, therefore no sliding failure occurs:** This assumption has been shown to be inappropriate; therefore it is necessary to use a more comprehensive limit analysis model such as that used in this investigation, which is able to take into consideration sliding at bag interfaces.
- **Blocks have infinite compressive strength:** The results from compression tests give a compressive strength of stabilised and unstabilised bags as 1.0 and 1.4 N/mm^2 respectively. The analysis software used was able to take this value into account to consider crushing failure of the arches, therefore removing this assumption from the model.
- **Blocks initially fit together perfectly:** Every effort was made to construct the arches accurately, and maintain a constant bag dimension, but there will inevitably be irregularities in the shape of the bags and the action of tamping that cause the contact area to vary at each interface. It is therefore difficult to know the exact contact area between each bag, nor how the area changes with increasing load. This assumption therefore is not true.

The distinctive behaviour of the stabilised earthbag arch has differentiated it from the other specimens, and suggests that plastic limit analysis could be appropriate for their analysis. One of the benefits of this is that material properties do not need to be determined. However, dimensions, including contact area, do need to be determined accurately. Due to the curvature and irregularity of the earthbag faces, the contact area does not extend to the full width of the bags. This results in a lower effective arch depth, and initial deformations upon load application, as the defects in the interfaces are smoothed out. These deformations can be significant enough to alter the overall geometry of the arch, which breaks another assumption of the model.

These factors show that either a factor needs to be brought in that somehow approximates the effective depth of the arch as a proportion of the bag width, or the model needs to be able to take into account the exact shapes of the bags. It is likely, however, that the exact shapes of the bags cannot be determined practically.

7 Discussion

These tests on earthbags have been conducted in a field with few experimental precedents or guidelines, and on a subject that is difficult to control and to define, in terms of unit size and material properties. These factors, along with a small experimental sample, made test repeatability and reliability of results an issue that needed to be considered.

There are many variables associated with earthbag structures, such as bag material, fill material, bag size, bag dimensions after tamping, to name just a few. There are no formal guidelines as to how to deal with these variables, so effort was made to control them in a way that would most closely replicate the conditions experienced in a real project, such as that discussed in Chapter 3. A similar fill material was chosen to that available on site; bag material and bag weight were kept consistent throughout the test programme.

One of the most difficult factors to control was the size of individual bags after tamping, as the exact amount of energy imparted into bags could not be controlled, nor would it be appropriate to try. The variation experienced in bag dimensions is predicted to be approximately 10%, but it was hoped that a representative average was used for calculations. This resulted in a variation in the number of bags required to build each arch, and could only be properly addressed by increasing the sample size of tests, which was unfortunately not possible in this programme.

7.1.1 Compression Tests

A single bag test was conducted in order to be able to compare results with those of Xu *et al* (2008), who obtained strong results that correlated very well with their theoretical predictions. However, our methodology must have varied due the experimental setup or component materials, as the values of strength were unattainable due to the strength of the sandbag exceeding the strength of the 200T testing frame. This is much greater than those results obtained by Xu *et al*, and was assigned largely to the friction between the bag and the loading plates. This prevented meaningful conclusions being drawn from this test, and demonstrates the difficulty in replicating tests on earthbags.

The accuracy of lateral displacement measurements on 8-bag stack compression tests was impacted by the overall rotation of the stacks upon application of load, which acted to cancel out the bulging of the individual bags. This is due to the difficulty of stacking the bags to fit perfectly and be level, due to their irregular and varied shape. The large deformations experienced also disrupted the tabs that were attached to the bags, from which displacement reading were taken. Therefore only readings from the initial parts of the test were used in the analysis, where the load-displacement behaviour was measured to be linear.

7.1.2 Arch Tests

There were no experimental precedents for this set of experiments that could be drawn upon to make comparison; therefore comparisons could only be made with theoretical predictions, which did not necessarily accurately model the behaviour of the arches. Due also to the difficulties mentioned above in controlling individual bag size, and the small sample size of tests, the repeatability of tests must be considered.

The only tests that were repeated were the earthbag shear tests, which were each conducted three times. These showed a strong repeatability with variation of only 2.5%, which was reassuring; although in these tests the bags area was controlled by the shearbox. Of the arch tests, Arch 2 and

Arch 5 are the most comparable, as the barbed wire was found to have little impact on the response of the arch to applied load. These show a relatively strong correlation, with variation of 6.5%, which suggests that test results are reliable and reasonable measures of control were undertaken in order to ensure test repeatability.

The large deformations experienced by the arches during testing made the consistent application of load difficult. The pin under the loading jack often rotated to its full extent, causing the load to be applied with a horizontal component. The rotation of the bags also meant that the location of the load varied slightly as the test progressed. In order to control these effects, the arches required unloading at intervals so that the load could be reset and spacers inserted under the jack. On at least one occasion, with Ach 3, as can be seen in Figure 6.6, the integrity of the arch was compromised due to this unloading after significant deformations had already occurred, and the peak load of the arch may have been affected by this action. Arch 3 also ultimately collapsed prematurely due to the further unloading of the structure, which affected the ultimate failure results.

8 Further Research

Flexible form rammed earth is a relatively new and untested construction method that could present an effective solution to many structural projects. Earthbag construction is a particularly effective building method for use in third world, disaster and emergency scenarios, and in order to utilise it to the maximum potential to create safe and efficient structures, it is important to conduct further research into the behaviour and feasibility of the system.

Building on from the work carried out in this paper, there are a number of particular areas that can be focused on in future work:

- **Efficacy of/Alternatives to barbed wire:** It has been suggested that from the findings of this paper, barbed wire offers little structural enhancement to an earthbag structure, but aides buildability. This claim could be investigated further, including three dimensional tests to take into account effects such as hoop stress. Contrastingly, if barbed wire's contribution is largely limited to ease of construction, other methods could perhaps be explored of achieving the same goal of stabilising earthbags during tamping.
- **Three dimensional tests**: One of the limitations of this paper has been the inability to test a full earthbag dome, and in doing so, take into account three dimensional effects such as hoop stress. A full structural test of an earthbag dome would demonstrate the full potential of the structural system, and could further develop the forms that can feasibly be achieved with this building method.

9 Conclusions

The material properties of an earthbag system using sand as fill material and polypropylene bags have been measured, and the strength of this system under compression and in a structural system has been tested.

It was found that earthbag structures are resilient structures that undergo large deformations before collapse, and exhibit highly plastic behaviour. When working with unstabilised fill material serviceability limit state is likely to govern design. In general, stabilised earthbags exhibit block-like behaviour at low stresses, and soil-like behave at stresses approaching peak stress. However, the precise dimensions of the blocks cannot be determined, which creates a level of uncertainty in the system and can generate higher than expected deformations, due to the irregularly shaped bag faces.

This investigation has also shown that, when fill material is stabilised, earthbag structures can be approximately modelled using plastic limit analysis that takes into account geometric factors, friction and crushing of bags. Consideration needs to be made, however, of the variability of individual earthbag dimension, and contact areas at bag interfaces, and the impact that this will have on effective arch depth and arch deformations.

When tested in this paper, barbed wire did not improve the structural performance of the earthbag system. Further tests need to be conducted on the contribution of barbed wire to the earthbag system in order to develop a more reliable and consistent picture of structural behaviour.

This paper has contributed to the growing foundation of knowledge on the behaviour of earthbag structures that is applying a scientific methodology to a relatively new and developing building method. It is hoped that this trend can continue, and that future work will be able to continue towards the goal of making earthbag structures a more efficient, viable solution to structural problems.

References

BS 1377-7 (1990). *Soils for Civil Engineering Purposes – Part 7: Shear Strength Tests (Total Stress).* BSI.
BS 13934-1 (1999). *Textiles — Tensile properties of fabrics — Part 1: Determination of maximum force and elongation at maximum force using the strip method.* BSI.
Cal-Earth (n.d). *About Cal-Earth* [online]. Available: http://calearth.org/about [22 April 2010].
Craig R. F. (2004). *Craig's Soil Mechanics.* 7th ed. Oxford: Taylor & Francis.
Daigle, B. (2008). *Earthbag Housing: Structural Behaviour and Applicability in Developing Countries.* Thesis (M.Sc.) Queen's University, Kingston, Ontario, Canada.
Dunbar, R. (2006). *Prism Test of Earthbags.* Undergraduate Research. West Point Military Academy.
Gilbert, M. and Melbourne, C. (1994). Rigid-Block Analysis of Masonry Structures. *The Structural Engineer,* 72 (21), pp.356-361.
Grasser K. and Minke G. (1990). *Building with Pumice.* Vieweg.
Hunter, K. and Kiffmeyer, D. (2004). *Earthbag building.* Canada: New Society Publishers.
Heyman, J. (1969). The safety of masonry arches. *International Journal of Mechanical Sciences,* 11 (4), pp.363-385.
Heyman, J. (1982). *The masonry arch*. Chichester: Ellis Horwood.
Heyman J. (1995). *The stone skeleton.* Cambridge: Cambridge University Press.
Khalili, N. (1990). Lunar, Martian and Asteroid Structures Built Insitu. *Engineering, Construction and Operations in Space II: Proceedings of Space 90.* 22-26 April 1990, Albuquerque, NM, USA. Albuquerque: ASCE, 1990, pp.779-789.
Khalili, N. and Vittore, P. (1998). Earth Architecture and Ceramics: The Sandbag/Superadobe/Superblock Construction System. *International Conference of Building Officials*, Cal-Earth Institute, Hesperia, CA, USA.
Khalili, N. (2008). *Emergency Sandbag Shelter and Eco-Village*. Hesperia: Cal-Earth Press.
LimitState (2009). Ring 2.0 [computer program]. Sheffield: LimitState.
Livesley, R. K. (1978). Limit analysis of structures formed from rigid blocks. *International Journal for Numerical Methods in Engineering,* 12 (12), pp.1853-1871.
Matsuoka, H. and Liu, S. (2006). *A new earth reinforcement method using soilbags.* London: Taylor & Francis.
Minke G. (2006). *Building with earth.* Basel: Birkhäuser.
du Pisanie, N. (2009). Communty Building - Sustainable, Appropriate Desert Building for the Topnaar Communities of the Kuiseb River. *11th International Conference on Non-Conventional Materials and Technologies,*6-9 September 2009, Bath. Bath: University of Bath.
Press.
Sinopoli, A. (1998). *Arch bridges*. Rotterdam: Balkerma.
Trivedi, B. (2002). Dirt Domes Designed for Emergency Housing. *National Geographic*, 3 April.
Vadgama, N. (2010). *A Material and Structural Analysis of Earthbag Housing.* Dissertation (M.Eng.). Bath University, Bath.
Anon, 2007. The Earthbag Architecture of Akio Inoue. *HomeDesign.com* [online], 4 February. Available: http://tiny.cc/earthbagarchitecture [22 April 2010].
von Willert, D. J. (1992). *Life strategies of succulents in deserts*. Cambridge: Cambridge University
Xu, Y., Jian, H., Yanjun, D. and De-an, S. (2008). Earth reinforcement using soilbags. *Geotextiles and Geomembranes,* 26 (3), pp.279-289.

Appendix A

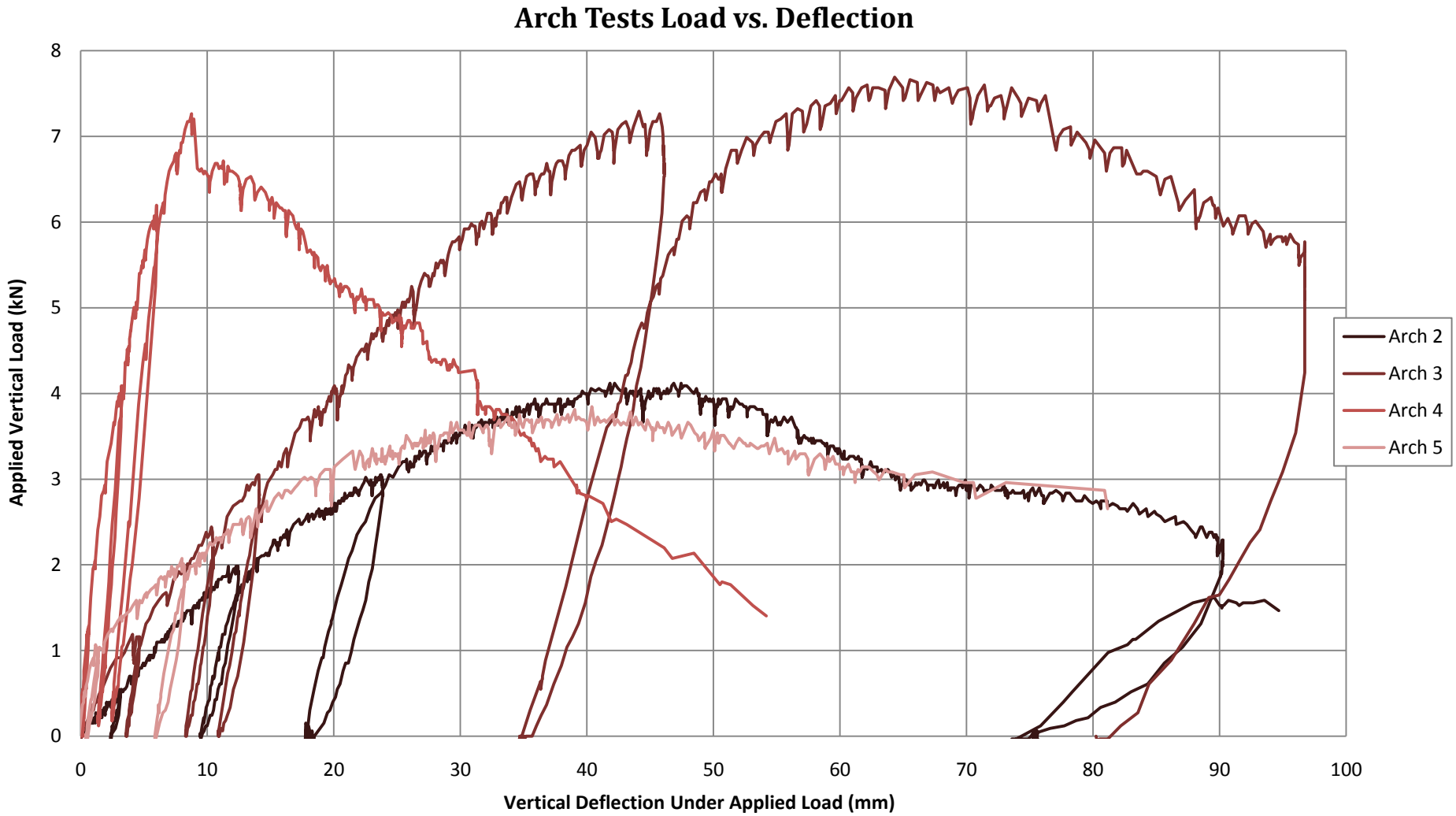

Figure A1: Graph showing arch test results of applied load against deflection under load.